MODELLING THE EXTRINSIC FINGER FLEXORS

MODELLING THE EXTRINSIC FINGER FLEXORS: TENDON EXCURSIONS AND MOMENT ARMS

By

AARON MICHAEL JOSEPH KOCIOLEK, B.Sc.

A Thesis

Submitted to the School of Graduate Studies

in Partial Fulfillment of the Requirements

for the Degree

Master of Science

McMaster University

MASTER OF SCIENCE (2009) McMaster University

(Kinesiology) Hamilton, Ontario

TITLE: Modelling the Extrinsic Finger Flexors: Tendon Excursions and Moment Arms

AUTHOR: Aaron Michael Joseph Kociolek, B.Sc. (Laurentian University)

SUPERVISOR: Dr. Peter Keir

NUMBER OF PAGES: xi, 100

ABSTRACT

A musculoskeletal model of the hand is needed to investigate the pathomechanics of tendon-related disorders and carpal tunnel syndrome. The purpose of this thesis was to develop a model with realistic extrinsic finger flexor tendon excursions and moment arms. An existing upper extremity model served as a starting point, which had programmed movement for the index finger. Movement capabilities were added to the middle, ring and little fingers. Metacarpophalangeal linkages were modelled as universal joints to simulate flexion/extension and abduction/adduction. Interphalangeal linkages were modelled as hinge joints to simulate flexion/extension. Extrinsic finger flexor tendon paths were modelled using two different approaches. The first method used control points fixed in the metacarpal and phalangeal coordinate systems to represent the annular and cruciate pulleys. The second method used wrapping surfaces at the metacarpophalangeal and interphalangeal joints to model constant moment arms with finger movement. Extrinsic finger flexor tendon excursions and moment arms in both the control point and joint wrapping models were iteratively adjusted to match the anthropometric regression model developed by Armstrong and Chaffin (1978) for a 50^{th} percentile male. Musculoskeletal scaling algorithms were also used to further evaluate the control point and joint wrapping models. More specifically, metacarpal and phalangeal segments were adjusted to determine the effects of length and thickness scaling on tendon kinematics. Tendon excursions and moment arms in the joint wrapping model best matched the anthropometric regression model. However, anatomical features

of the tendons paths at the finger joints were not preserved in the joint wrapping model as noted by ultrasound imaging. Depending on user needs, both anatomic fidelity and model outcomes should be considered as compromises may be necessary in the modelling process.

ACKNOWLEDGEMENTS

I would like to thank my thesis advisor Dr. Peter Keir. His door was always open whenever I needed help. He always had patience for me. Also, he allowed this project to be my own while directing me down all the right paths. Most importantly, he always had confidence in my abilities, which pushed me to be a better student.

I am thankful to Dr. Maureen MacDonald. She provided me with an opportunity to collect ultrasound images of the finger flexor tendons. She was willing to spend time with me in her research lab to perfect the experimental protocol for this thesis.

I am grateful for the support of my lab mates Joshua Cashaback, Kia Sanei, Marty Smets, Justin Weresch, Daniel Avrahami, Joanne Hodder, Tara Kajaks and Mike Holmes. Their friendship made this experience much, much easier.

I would especially like to thank my Mom and Dad (Micheline and John) for always believing in me. I am so blessed to have such kind and loving parents who devoted their lives to making mine better. And, I owe many thanks to the rest of my family for their unconditional love.

Lastly, I have to thank the love of my life and my best friend Allyson. She stood by me throughout this thesis. She makes me a better person.

TABLE OF CONTENTS

LIST OF TABLES

LIST OF FIGURES

CHAPTER 1 – INTRODUCTION

Work-related musculoskeletal disorders (WMSDs) of the upper extremity represent the second most frequent lost-time claim in Ontario. From 1995 to 2005, thirty percent of all reported disorders involved soft tissue damage at the shoulder, arm, elbow, wrist and hand (WSIB, 2006). While there is epidemiological evidence of a relationship between ergonomic risk factors and disorders of the distal upper extremity, the underlying pathomechanics are not well understood. A common pathological finding in patients with wrist and hand tendinopathies and carpal tunnel syndrome (CTS) is non-inflammatory fibrosis and thickening of the subsynovial connective tissue (SSCT) that surrounds the flexor digitorum profundus (FDP) and flexor digitorum superficialis (FDS) tendons (Barr et al., 2004). These histological observations are characteristic of degeneration due to repeated mechanical stress (Schuind et al., 1990). Also, pathological changes to the SSCT are most evident close to the finger flexor tendons, which suggest that shear forces are involved in distal upper extremity injury mechanisms (Armstrong et al., 1984). In a recent study, relative motion between the FDS and SSCT was measured in cadavers with and without a history of CTS (Ettema et al., 2008). The cadavers with CTS had increased adherence or dissociation between the tendons and SSCT compared to the healthy controls. Similar findings were also documented in other studies (Yamaguchi et al., 2008; Yoshii et al., 2008; Ettema et al., 2007; Ugbolue et al., 2005; Szabo et al., 1994). Changes in tendon gliding might further increase frictional forces resulting in a viscous cycle of degradation (Ettema et al., 2006a; 2006b).

Changes in tendon kinematics within the carpal tunnel might also increase frictional work (the product of displacement and shear force) between the FDP, FDS, median nerve (MN) and transverse carpal ligament (TCL). Zhao et al. (2007) constructed an apparatus to measure gliding resistance of the tendons that pass through the carpal tunnel in cadaveric specimens. Load cells were connected at the proximal and distal ends of the FDS tendon for the middle finger and a mechanical actuator simulated finger flexion/extension cycles at 20 Hz in different wrist postures. The researchers showed that gliding resistance increased when the middle finger was moved alone (compared to all fingers moved together). The highest mean and peak gliding resistances were 0.2 ± 0.05 N and 2.5 ± 1 N, which occurred at 60° wrist flexion while moving the middle finger alone. Further research is required to study gliding resistance in cadavers with WMSDs. Moore et al. (1991) developed a 2-dimensional model for calculating tendon frictional work as part of a method for quantifying injury risk. The researchers showed that frictional work estimates in the laboratory were highly correlated with upper extremity injury statistics in an epidemiology study by Silverstein et al. (1987) using similar task definitions to quantify force and frequency. The development of a three-dimensional musculoskeletal model for calculating differential tendon motion and frictional work might be important in further studying pathomechanics of wrist and hand tendinopathies and CTS.

Several researchers have measured FDP and FDS tendon excursions with different wrist and finger movements using both *in vitro* (Ettema et al., 2008; 2007; Yamaguchi et al., 2008; Ugbolue et al., 2005; Netscher et al., 1998; 1997; Horii et al.,

1993; 1992; Szabo et al., 1994; Minamikawa et al., 1992; An et al., 1983; Armstrong and Chaffin, 1978; Brand et al., 1975) and *in vivo* (Lopes, 2007; Oh et al., 2007; Erel et al., 2003; Dilley et al., 2001; Hough et al., 2000; Buyruk et al., 1998; Cigali et al., 1996) study methods. Armstrong and Chaffin (1978) evaluated extrinsic wrist and finger flexor excursions in 4 hand cadavers using a micrometer to measure tendon displacement and a camera to obtain joint angles. These data were used to develop anthropometric-based regression models for predicting tendon excursions. More specifically, the inputs for these equations were joint thicknesses and postures. An et al. (1983) also showed that tendon excursions were dependent on joint thicknesses in a cadaver study of the index finger. More recently, researchers have used ultrasound to measure tendon excursions *in vivo*. Lopes (2007) measured FDS tendon motion in 16 healthy and 6 cumulative trauma disorder participants. Tendon excursions for the symptomatic group were not different compared to healthy participants, which might be due to the small sample population as well as variations in the disorders. However, tendon excursions obtained with spectral Doppler ultrasound were large compared to the regression model developed by Armstrong and Chaffin (1978). These discrepancies might be due to cadaveric methods in previous studies. Still, further research is required to validate FDP and FDS tendon excursions from ultrasound.

Biomechanical models have great potential for studying the musculoskeletal system. Several hand models have been developed to study muscular coordination and joint loading (Wu et al., 2009; Mogk and Keir, 2007; Holzbaur et al., 2005; Li et al., 2000; Valero-Cuevas et al., 1998; Leijnse et al., 1993; 1992; An et al., 1979). Holzbaur

et al. (2005) recently developed a three-dimensional model of the upper extremity, which simulates movement at the shoulder, elbow, forearm, wrist, thumb and index finger. However, movement capabilities of the middle, ring and little fingers with realistic FDP and FDS excursions are required in order to further study differential tendon motion and develop a three-dimensional model for calculating frictional work.

1.1. Purpose

The objectives of this thesis were to:

1. add movement capabilities of the middle, ring and little fingers in the Holzbaur et al. (2005) upper extremity model, including metacarpophalangeal (MCP) flexion/extension and abduction/adduction, proximal interphalangeal (PIP) flexion/extension and distal interphalangeal (DIP) flexion/extension;
2. model extrinsic finger flexors using tendon excursions and moment arms from Armstrong and Chaffin (1978) for a 50^{th} percentile male;
3. determine the effects of anthropometrical scaling on tendon excursions and moment arms;
    a. measure external hand dimensions (including joint thicknesses) and moment arms (using ultrasound) in three participants to further evaluate the current musculoskeletal models.

CHAPTER 2 - REVIEW OF LITERATURE

2.1. Work-Related Musculoskeletal Disorders of the Distal Upper Extremity

Work-related musculoskeletal disorders include injuries to muscles, tendons, nerves and supporting structures that generally develop over time due to repetitive loading (Zakaria et al., 2004). Typical disorders of the distal upper extremity include tendinitis, tenosynovitis, tendinosis and peripheral neuropathy (Tanaka et al., 2001). Tendinitis is as an acute tendon condition characterized by inflammation and pain (Khan et al., 1999). Tenosynovitis also involves an inflammatory response, but to the synovial sheath that surrounds a tendon (Khan et al., 1999). Conversely, tendinosis is a chronic condition characterized by cumulative degeneration of the tendon due to inadequate repair, which occurs in the absence of inflammation (Khan et al., 1999). A peripheral neuropathy describes any damage to the peripheral nervous system, due to mechanical compression (Zakaria, 2004).

In the province of Ontario, upper extremity WMSDs represent the second most frequent injury claim, only to the lumbar spine (WSIB, 2006). A total of 975,400 lost time disorders were reported between 1996 and 2005. Thirty percent of these claims involved soft tissue injuries at the shoulder, arm, elbow, wrist and hand (WSIB, 2006). Furthermore, disorders of the upper extremity are generally more expensive to repair and rehabilitate compared to other body regions including the lumbar spine (Silverstein et al., 1998).

Several epidemiology studies have also quantified workplace injury rates of the distal upper extremity. Gerr et al. (2002) showed that the annual incidence rate of forearm and hand WMSDs was 2.2 ± 2.6 occurrences per 100 computer workers. In another study, the incidence of flexor tendinitis in four industrial and three clerical workplaces was 24.3% over 5.4 years or 4.5% annually (Werner et al., 2005). Furthermore, workers with flexor tendinitis are more likely to develop CTS in time (Manktelow et al., 2004).

Carpal tunnel syndrome is the most frequent peripheral neuropathy in the workplace (Zakaria, 2004). Symptoms of CTS include pain, numbness and tingling in the index and middle fingers of the hand. These symptoms are often present at night or with physical activity, and in severe cases patients can lose function in their hands (Rettig, 2001). An epidemiology study of 632 computer users estimated that the annual incidence of CTS was 0.5 ± 0.3% (Gerr et al., 2002). In 1996, a total of 964 workers registered with the Workplace Safety and Insurance Board of Ontario were diagnosed with CTS (Manktelow et al., 2004). Seventy-five percent of these workers received surgery and returned to the workplace, on average, three months later. The cost to the WSIB was greater than $13,200,000 (or $13,700 per worker) each year between 1996 and 2000. Furthermore, a follow-up survey in 2000 revealed that 47% of these workers still experienced severe pain and only 14% had no symptoms related to CTS.

2.2. Ergonomic Risk Factors and Work-Related Musculoskeletal Disorders

2.2.1. Posture and Work-Related Musculoskeletal Disorders

Epidemiology studies suggest that there is a relationship between extreme wrist and hand postures and flexor tenosynovitis (Luopajärvi et al., 1979) and CTS (Tanaka et al., 1995; Moore and Garg, 1994; de Krom et al., 1990). Luopajärvi et al. (1979) showed that extreme work postures increased the risk of flexor tenosynovitis by a factor of 4.1 in assembly line workers compared to shopping assistants. Odds ratios (that compare hazardous to safe jobs categorized by posture observations and self reports) were also calculated for CTS with values between 2.8 (Moore and Garg, 1994) and 5.9 (Tanaka et al., 1995).

Biomechanical studies also suggest that posture is a risk factor in the development of CTS. Keir et al. (1997) measured carpal tunnel pressure with a pressure transducer connected to a catheter inserted percutaneously in cadaveric specimens. Several wrist postures were tested including nine in the flexion/extension plane and five in the radial/ulnar deviation plane. Carpal tunnel pressure increased with wrist flexion and extension as well as radial and ulnar deviation. Weiss et al. (1995) measured carpal tunnel pressure using a similar catheter technique in 24 participants. Wrist postures were measured concurrently with an electrogoniometer. Carpal tunnel pressure had a parabolic relationship with increased joint angles in the wrist flexion/extension plane. Researchers also showed that carpal tunnel pressure was dependent on forearm pronation/supination (Rempel et al., 1998). The lowest pressure was at 45° pronation and increased significantly near the extremes of both pronation and supination. In another study, carpal

tunnel pressure was greater during pinching compared to simple finger pressing (Keir et al., 1998).

Furthermore, awkward work postures including extreme wrist flexion or extension, radial or ulnar deviation and pinching also increase muscle activations of the extrinsic wrist and finger flexors (Keyserling, 2000). The flexor tendons are subjected to tension when the wrist and fingers are in a neutral position. However, when the wrist and fingers are flexed the tendons also endure compression and shear forces as they slide past other structures in the carpal tunnel (Keyserling, 2000).

2.2.2. Force and Work-Related Musculoskeletal Disorders

There is strong epidemiological evidence of a positive relationship between force and flexor tendinitis and CTS (NIOSH, 1997). Workers that perform forceful tasks are 4.8 times more likely to develop flexor tendonitis (Armstrong et al., 1987) and 2.8 (Moore and Garg, 1994) to 15.5 (Silverstein et al., 1987) times more likely to develop CTS than those who do not. Moreover, biomechanical studies show that carpal tunnel pressure increases with fingertip load in the absence of other risk factors including posture and repetition (Keir et al., 1998; 1997; Rempel et al., 1997). Even small fingertip forces (5 – 15 N) increased carpal tunnel pressure (Keir et al., 1998).

2.2.3. Repetition and Work-Related Musculoskeletal Disorders

Highly repetitive work tasks are associated with flexor tendinitis and CTS (NIOSH, 1997). Silverstein et al. (1987) divided 652 workers with 39 different jobs into high and low repetition groups based on measurements of wrist motion and cycle time. The researchers found that that the prevalence of CTS was 5.5 times greater in the high

repetition group (compared to the low repetition group). Biomechanists have also studied the effects of repetition in the workplace. Szabo and Chidgey (1989) measured carpal tunnel pressure in 28 participants during passive wrist flexion/extension movements at a rate of 30 cycles per minute for one minute. Carpal tunnel pressure was increased immediately following the wrist movement protocol. Marras and Schoenmarklin (1993) measured dynamic wrist motions, including velocities and accelerations, in high and low risk injury groups defined by ergonomists. Greater wrist accelerations and velocities were observed in the high risk group. The researchers also suggested that high wrist accelerations are responsible for increasing tendon shear with other structures in the carpal tunnel, which in turn causes injury.

2.2.4. Posture, Force and Repetition and Work-Related Musculoskeletal Disorders

While there is epidemiological evidence that posture, force and repetition are all independently associated with flexor tendinitis and CTS, a stronger relationship exists when these factors occur simultaneously (NIOSH, 1997). From a biomechanical perspective, this finding is expected since these risk factors increase tendon displacement and shear forces, which multiplied together, is frictional work (Sommerich et al., 1996). Moore et al. (1991) developed a two-dimensional model of the finger to estimate frictional work on the tendon. Estimates of frictional work in the laboratory were highly correlated with upper extremity injury statistics in an epidemiology study by Silverstein et al. (1987) using similar task definitions to quantify force and frequency. The researchers suggested that these calculations could be used to predict injury potential since this measure is sensitive to changes in posture, force and repetition. However, a

three-dimensional musculoskeletal model with realistic FDP and FDS tendon excursions (and the potential to add frictional components) is needed to further study injury mechanisms (Mogk and Keir, 2007).

2.3. Anatomy of the Carpal Tunnel

A transverse section of the carpal tunnel at the hamate level illustrates the structures found within this small space (Figure 2.1). The dorsal carpal tunnel consists of 8 carpal bones in 2 rows (proximal row – scaphoid, lunate, pisiform and triquetrum; distal row – trapezium, trapezoid, capitate and hamate) that are covered by the volar wrist capsule (Rettig, 2001). The TCL shapes the roof of the carpal tunnel, which is attached to the tubercle of the trapezium radially and to the hook of the hamate ulnarly. The MN and nine flexor tendons pass through the carpal tunnel. The flexor pollicis longus (FPL) tendon is located close to the radial wall in the carpal tunnel. The FDS tendons are in the volar aspect of the carpal tunnel and the FDP tendons are located more dorsally in this space. The flexor tendons are cushioned from the carpal bones with two bursae including a radial bursa for the FPL tendon and an ulnar bursa for the FDS and FDP tendons. Subsynovial connective tissue is situated in the carpal tunnel between the flexor tendons and the single celled visceral synovial layer (Ettema et al., 2007).

2.4. Anatomy of the Hand

The hand is comprised of 8 carpals, 5 metacarpals, and 14 digital bones (including the proximal and distal thumb phalanges and the proximal, middle and distal finger

phalanges) that form intercarpal, carpometacarpal, metacarpophalangeal, and interphalangeal joints (Marieb, 2003). The extrinsic finger flexors include the FDP and FDS (Table 2.1). Five ligamentous thickenings of arcing fibres (annular pulleys) constrain the FDP and FDS tendon paths (Figure 2.2). Additional thin criss-crossing fibres (cruciate pulleys) that constrain the tendons are also located at the interphalangeal joints between the annular pulleys. These pulley systems prevent bowstringing of the tendons during MCP, PIP and DIP flexion. The annular and cruciate pulleys also minimize tendon displacements during finger movements (Goodman and Choueka, 2005). The extrinsic finger extensors include the extensor digitorum communis and extensor indicis proprius. The extensor digitorum communis does not have completely separated muscle bellies (Brand and Hollister, 1985). Also, inter-digit tendinous connections exist proximal to the MCP joints (Chao and An, 1989). These features limit the ability of the individual extensor digitorum musculotendon units to function independently (Leijnse et al., 1993; 1992).

The intrinsic hand muscles include the lumbricals and palmar and dorsal interossei. The lumbricals are tiny worm-like muscles with origins on the deep flexor tendons and assist with MCP flexion while maintaining PIP and DIP extension. The palmar and dorsal interossei originate from the metacarpal sides and allow for MCP adduction and abduction, respectively. The interossei muscles also assist with PIP and DIP extension. The lumbricals and interossei insert with the extensor digitorum tendons into the extensor expansion (a tendinous aponeurosis on the dorsal metacarpals and phalanges). However, anatomical descriptions of the lumbricals and interossei are

typically oversimplified. In reality, multiple insertions of the lumbricals and interossei frequently exist with a high level of anatomic variability (Eladoumikdachi et al., 2002a; 2002b).

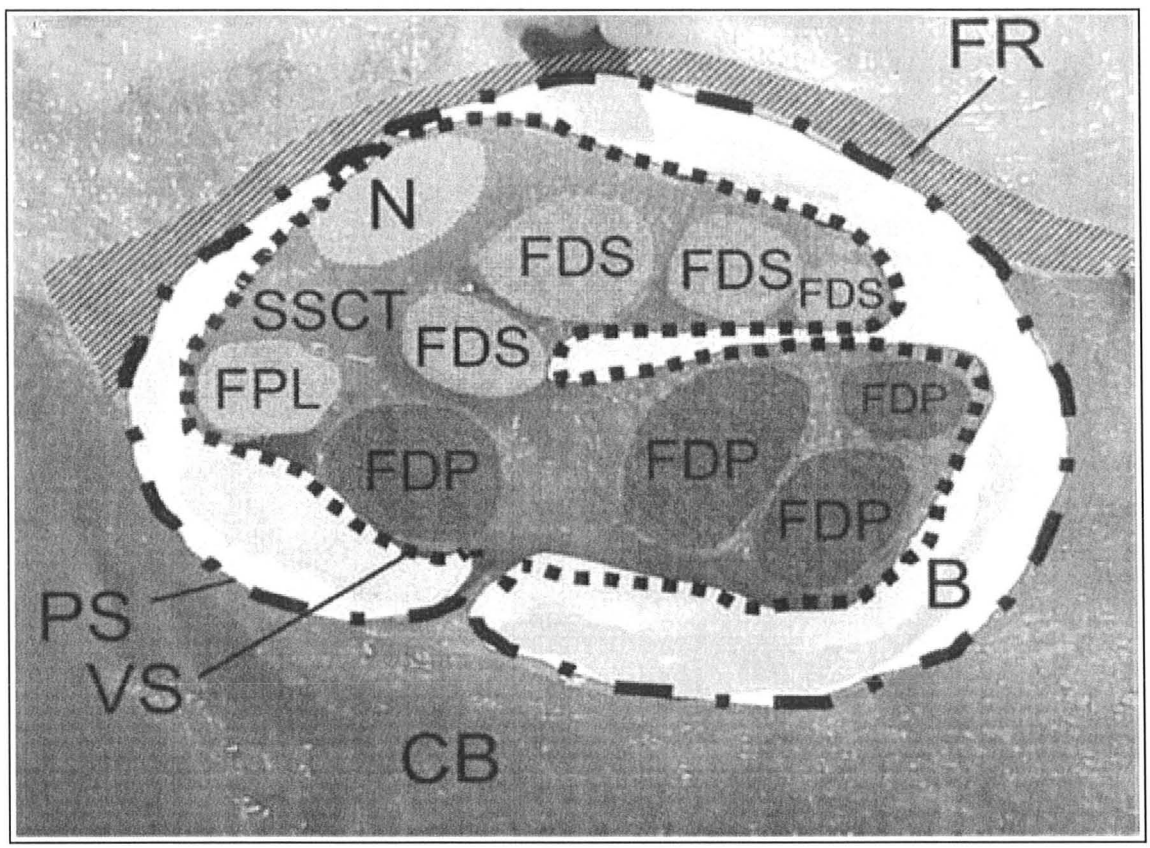

Figure 2.1. Transverse section of the carpal tunnel at the level of the hamate (FR – flexor retinaculum; CB - carpal bones; N - median nerve; FPL - flexor pollicis longus tendon; FDP - flexor digitorum profundus tendons; FDS – flexor digitorum superficialis tendons; B – bursae; SSCT - subsynovial connective tissue; PS - parietal synovial layer; VS - visceral synovial layer). From Ettema et al., 2007 (page 293).

Table 2.1. Extrinsic and intrinsic muscles that control movement of index, middle, ring and little fingers. From Marieb, 2003 (pages 358-366).

Muscle	Origin	Insertion	Action
	Extrinsic Finger Flexors and Extensors		
Flexor Digitorum Profundus	Anteromedial surface and coronoid process of ulna; Interosseous membrane	By four tendons into distal finger phalanges	Flexes wrist; Flexes MCP, PIP and DIP joints of fingers
Flexor Digitorum Superficialis	Medial epicondyle of humerus; Coronoid process of ulna; Shaft of radius	By four tendons into middle finger phalanges	Flexes wrist; Flexes MCP and PIP joints of fingers
Extensor Digitorum Communis	Lateral epicondyle of humerus	By four tendons into the extensor expansion of fingers	Extends wrist; Extends MCP, PIP and DIP joints of fingers
Extensor Indicis Proprius	Posterior surface of distal ulna; Interosseous membrane	Extensor expansion of index finger	Extends wrist; Extends index finger
	Intrinsic Hypothenar Muscles of the Little Finger		
Abductor Digiti Minimi	Pisiform	Medial side of proximal little finger phalanx	Abducts little finger at MCP joint
Flexor Digiti Minimi Brevis	Hamate and TCL	Medial side of proximal little finger phalanx	Flexes little finger at MCP joint
Opponens Digiti Minimi	Hamate and TCL	Medial side of little finger metacarpal	Opposition (brings metacarpal of little finger toward thumb)
	Intrinsic Midpalmar Muscles		
Lumbricals	Lateral side of flexor digitorum profundus tendons in palm	Lateral edge of extensor expansion at proximal finger phalanges	Flexes MCP joints and extends PIP and DIP joints of fingers
Palmar Interossei	Side of metacarpals facing hand mid-axis	Extensor expansion of proximal finger phalanges	Adducts MCP joints of fingers; Assists lumbricals
Dorsal Interossei	Sides of metacarpals	Extensor expansion of proximal finger phalanges	Abducts MCP joint of fingers; Assists lumbricals

* MCP – metacarpophalangeal; PIP – proximal interphalangeal; DIP – distal interphalangeal; TCL – transverse carpal ligament

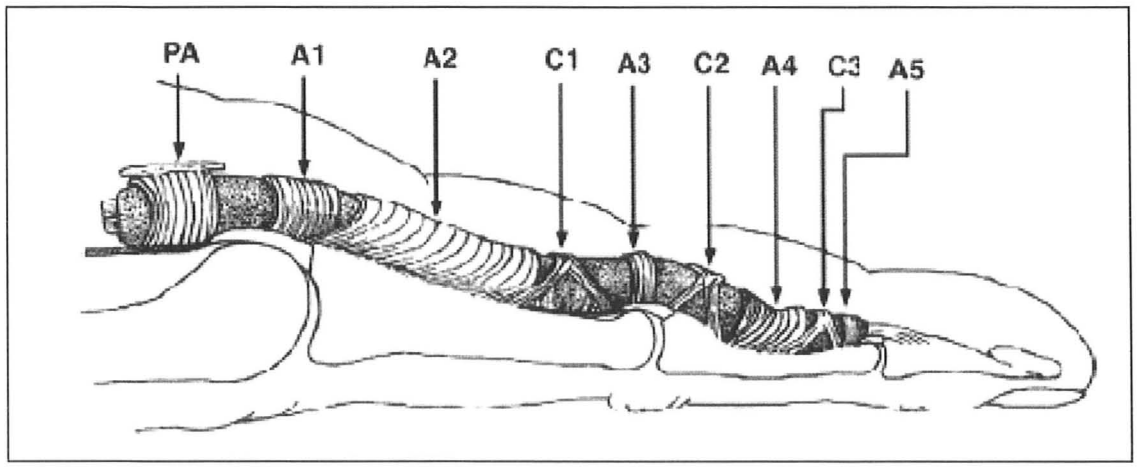

Figure 2.2. Pulley systems in the finger (PA – palmar apaneurosis pulley; A1 to A5 – annular pulleys; C1 to C3 – cruciate pulleys). From Goodman and Choueka, 2005 (page 135).

2.5. Mechanisms of Work-Related Musculoskeletal Disorders

Even though current research clearly demonstrates a relationship between ergonomic risk factors (including posture, force and repetition) and WMSDs of the distal upper extremity, the exact pathomechanics for many of these conditions are unknown. The complexities of various causes and risk factors as well as the diversity of signs and symptoms present many challenges to studying distal upper extremity WMSDs. It is generally accepted that CTS results directly or indirectly from increased carpal tunnel pressure, which causes compression of the median nerve. Weiss et al. (1995) measured carpal tunnel pressure in 4 patients with CTS and 20 healthy control participants. The researchers demonstrated that carpal tunnel pressure was twice as high in the CTS patients (19 ± 2mmHg) compared to controls (8 ± 4mmHg). Szabo and Chidgey (1989) also found that carpal tunnel pressure was higher in patients with CTS (compared to healthy participants).

Pressure in the carpal tunnel can increase if the size of the canal decreases or the contents in this space increase (Ettema et al., 2007). The most frequently reported pathological finding in patients with wrist and hand tendinopathies and CTS is non-inflammatory fibrosis and thickening of the SSCT (Barr et al., 2004). The SSCT wraps around FDP and FDS tendons in the carpal tunnel (Ettema et al., 2004). It is comprised of collagen bundles parallel to the tendons, which are coupled together by smaller collagen fibres arranged vertically (Ettema et al., 2006a; 2006b). During finger movement, the SSCT is stretched and the bundles move one at a time due to the vertical connections (Ettema et al., 2008; 2007). In this manner, the tendons slide in their sheaths producing movement (Figure 2.3). Histological changes to the SSCT are characteristic of degeneration due to repeated mechanical stress (Schuind et al., 1990). Also, these changes are most evident close to the finger flexor tendons, which suggest that shear forces are involved in distal upper extremity injury mechanisms (Armstrong et al., 1984).

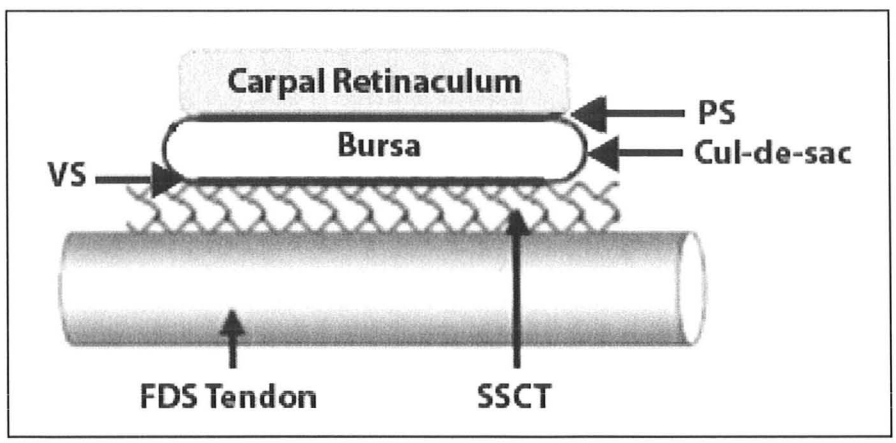

Figure 2.3. Sliding unit of the finger flexors in the carpal tunnel (FDS – flexor digitorum superficialis; SSCT – subsynovial connective tissue; PS – parietal synovium; VS – visceral synovium). From Ettema et al., 2008 (page 293).

In order to determine if fibrosis of the synovium influences extrinsic finger flexor tendon gliding, investigators used a digital camera to measure FDS and SSCT movement in cadaveric specimens with and without a history of CTS (Ettema et al., 2008). The measurements from cadavers with CTS revealed two separate patterns compared to healthy controls. One group had increased adherence between the tendon and the SSCT. Another group had increased dissociation between the tendon and the SSCT. The researchers suggested that fibrosis of the SSCT results in tethering between the tendon and visceral synovium. The mechanical changes in the carpal tunnel likely result in pressure redistribution. Consequently, the tendon and visceral synovium begin to move independently from each other. Changes in tendon gliding might further increase frictional forces resulting in a viscous cycle of degradation (Ettema et al., 2006a; 2006b).

Researchers have also measured shear forces in the carpal tunnel. Shear forces between the extrinsic finger flexors tendons and their sheaths are generally less than 0.1N (Amadio, 2005). The corresponding coefficient of friction between these two structures is less than 0.05. Still, these forces might assist in the development of flexor tenosynovitis and CTS (Rettig, 2001). In a recent study, researchers measured the relative motion between the FDS and SSCT using fluoroscopy in order to calculate a shear index, which was defined as the difference in motion between the two tissues relative to the tendon (Yoshii et al., 2008). While this approach was used to demonstrate the advantages of carpal tunnel release, further studies are required to evaluate the effects of injury on tendon movement and gliding resistance.

The initial development of a distal upper disorder might result in more friction, due to damage at the surfaces of the tendons and synovial sheath as well as the annular and cruciate pulley systems (Amadio, 2005). Uchiyama et al. (1995) constructed an apparatus to measure FDP tensions on each side of the A2 pulley during tendon gliding. More specifically, two load cells were connected in series with the FDP tendon (one on each side of the A2 pulley) and a mechanical actuator was used to generate displacements. The difference in measured tendon tensions was used to calculate friction. The frictional forces in 9 healthy cadaveric specimens at the FDP A2 pulley interface were between 0.021 and 0.031 N. The corresponding coefficients of friction were between 0.022 and 0.063.

Shear forces between the FDP and FDS tendons, the MN and other carpal tunnel structures (such as carpal bones, bursae and the TCL) most likely contribute to the development of flexor tendinitis and CTS (Szabo et al., 1994). Recently, researchers quantified mean and peak gliding resistance of the middle finger FDS tendon within the carpal tunnel (Zhao et al., 2007). Load cells were connected at the proximal and distal ends of tendon to calculate frictional forces and a mechanical actuator simulated finger flexion/extension cycles at 20 Hz. Eight cadaver hands were tested in five different wrist positions (including 60° flexion, 30° flexion, 0°, 30° extension and 60° extension) while moving all finger together and moving the middle finger alone. The highest mean and peak gliding resistances occurred at 60° flexion while moving the middle finger alone, which were 0.2 ± 0.05 N and 2.5 ± 1 N, respectively. This study suggests that a model

for calculating frictional work might be important in understanding the pathomechanics of distal upper extremity WMSDs.

2.6. Tendon Excursions

2.6.1. In Vitro Tendon Excursion Measurements

Several researchers have evaluated FDP and FDS excursions *in vitro* using potentiometers to measure tendon displacement and motion capture systems to obtain corresponding joint angles (Ettema et al., 2008; 2007; Yamaguchi et al., 2008; Ugbolue et al., 2005; Netscher et al., 1998; 1997; Horii et al., 1993; 1992; Szabo et al., 1994; Minamikawa et al., 1992; An et al., 1983; Armstrong and Chaffin, 1978; Brand et al., 1975). Armstrong and Chaffin (1978) determined the effects of hand anthropometry on tendon excursions using 4 healthy cadaveric hand specimens. The cadavers were secured to a steel frame and FDP and FDS tendons were fixed to a displacement micrometer one at time. The tendons were displaced in 2.5 mm increments while maintaining 2 N of tension. The joint positions were photographed at each increment in the flexion/extension plane. In order to measure the tendon excursion associated with each wrist and finger joint independently, splints were used to lock the other joints of noninterest. Using these measurements, the researchers developed linear regression equations to predict tendon excursions from joint thicknesses and postures (equations 2.1 and 2.2). The regression models accounted for more than 95% of variance observed in measured excursions.

An et al. (1983) measured both extrinsic and intrinsic tendon excursions at the index finger in seven cadaveric hand specimens using similar measurement techniques. Tendon excursions were measured with each MCP flexion/extension and abduction/adduction, PIP flexion and DIP flexion. Moment arms of the index finger muscles were also derived using a geometrical tendon pulley model developed by Landsmeer (1960). The researchers also showed that FDP and FDS tendon excursions and moment arms were highly correlated with joint thicknesses during finger flexion/extension.

$$\text{Wrist tendon excursion (mm)} = 0.0263W_1 + 0.005W_1W_2 + 0.106W_1W_3 - 0.000960W_1W_2W_4 \quad (2.1)$$

where, W_1 = joint angle (°) from neutral wrist position ($W_1 > 0°$ wrist flexion);
W_2 = joint thickness (mm);
W_3 = 0 for extension; 1 for flexion;
W_4 = 0 for superficialis; 1 for profundus.

$$\text{Finger tendon excursion (mm)} = 0.1034X_5 + 0.004211X_4X_5 - 0.0162X_3X_5 - 0.03043X_1X_5 - 0.06818X_2X_5 + 0.03679X_1X_3X_5 \quad (2.2)$$

where, X_1 = 1 for proximal interphalangeal joint; 0 for other joints;
X_2 = 1 for the distal interphalangeal joint; 0 for other joints;
X_3 = 1 for the profundus tendon; 0 for the superficialis tendon;
X_4 = joint thickness (mm);
X_5 = joint angle (°) from straight finger.

Several other researchers have measured extrinsic wrist and finger flexor tendon excursions in cadaveric hand specimens. Horii et al. (1992) showed that extrinsic finger flexor excursions increased with tendon load during PIP and DIP flexion. Netscher et al. (1998) showed that FDP and FDS tendon excursions increased following endoscopic release of the TCL. In another study, researchers evaluated the effects of pulley advancement at that MCP joint on FDP and FDS tendon excursions (Brand et al., 1975). Pulley advancement increased excursions with MCP flexion. Minamikawa et al. (1992) measured extrinsic wrist and finger extensor excursions in the index finger to evaluate various passive motion exercises following the repair of severed tendons. Other researchers have measured the relative motions of the FDP, FDS, MN and SSCT to determine stereotypical patterns in injured tendons, which might be related to physiological changes of the synovium (Ettema et al., 2008; 2007; Yamaguchi et al., 2008; Ugbolue et al., 2005; Szabo et al., 1994).

2.6.2. In Vivo Tendon Excursion Measurements

Several researchers have measured tendon excursions *in vivo* using ultrasound methods (Lopes, 2007; Oh et al., 2007; Erel et al., 2003; Dilley et al., 2001; Hough et al., 2000; Buyruk et al., 1998; Cigali et al., 1996). The use of ultrasound imaging for diagnosing musculoskeletal injuries in the clinical setting is increasing in popularity due to accessibility, examination time and costs (Beekman et al., 2003). Furthermore, ultrasound can be used to quantify both static and dynamic measures including moment arms and tendon excursions. Typical ultrasound procedures involve transmitting ultrasonic waves into musculoskeletal tissues using a high-frequency linear array

transducer between 7 – 12 MHz (Beekman et al., 2003). As ultrasonic waves arrive at a boundary between two different types of tissue, they are reflected back to the transducer. Dilley et al. (2001) captured high-frequency ultrasound images at 10Hz and calculated FDP and MN displacements using cross-correlation analysis in sequential frames. Tendon excursions with 30° of passive index finger extension were between 5.73 - 20.81 mm. The researchers also demonstrated that this method was accurate and reliable at low tendon velocities (1 - 10 mm/s) in a series of control phantom experiments (using 3-ply string with 2.5 mm diameter). However, further validations with the extrinsic wrist and finger flexor tendons are required.

Researchers have also used spectral Doppler ultrasound to obtain velocity-time curves for the tendons in the carpal tunnel. The integral of velocity is calculated to determine tendon excursion. Lopes (2007) used spectral Doppler ultrasound to calculate FDS and MN displacements in 16 healthy and 6 self-identified cumulative trauma disorder participants. Five wrist and finger movements were tested including wrist flexion, MCP flexion, full finger flexion, wrist and full finger flexion and pinching. Tendon excursions in the symptomatic group were not different compared to healthy participants. However, this study was limited by the small symptomatic sample population as well as variations in the self-reported disorders. Lopes (2007) also showed that tendon excursions in the spectral Doppler ultrasound study were considerably larger than the anthropometric regression models developed by Armstrong and Chaffin (1978). While these discrepancies might be due to cadaveric measurement methods in earlier

studies, further research is required to validate tendon excursions using spectral Doppler ultrasound.

In another study, colour Doppler imaging was used to measure velocities of the middle finger FDS and SSCT in cadaver hands with a history of CTS (Oh et al., 2007). The researches demonstrated that the ratio of FDS to SSCT velocity increased with faster finger flexion movements. Buyruk et al. (1998) used both colour Doppler imaging and displacement micrometer methods to obtain FDP and FDS tendon excursions in cadaveric specimens during passive finger flexion. Tendon excursions obtained from colour Doppler imaging were highly correlated with the micrometer technique. Other studies have also demonstrated that colour Doppler imaging methods are accurate and reliable (Erel et al., 2003; Hough et al., 2000; Cigali et al., 1996).

2.6.3. Tendon Excursion Models

Although numerous studies have documented FDP and FDS displacements, models that relate joint postures with tendon excursions are in short supply. Landsmeer (1960) developed a series of models to calculate tendon excursions for three possible joint configurations. In the first model, the tendon is located on the curve of the proximal bone articular surface (Figure 2.4a). This anatomical configuration is mathematically described by equation 2.3, where x is tendon excursion, r is the distance from the joint centre to the tendon and θ is joint displacement. The second model describes an anatomical situation where the tendon is tethered at a single point so that an infinite radius of curvature exists at the joint (Figure 2.4b), which is described by equation 2.4. The third model represents a tendon that is curved at the joint by an annular pulley

(Figure 2.4c). This is mathematically described by equation 2.5, where y is the distance from the joint centre to the tendon and d is the distance from the bone shaft to the tendon.

Armstrong and Chaffin (1978) evaluated the efficacy of these geometrical models at the wrist and finger joints for both FDP and FDS. Landsmeer's first model explained the most variance in tendon excursions 58% of the time. This model also appears to best represent the anatomical configuration of the wrist and finger joints (Armstrong and Chaffin, 1978). While there is good agreement between experimental and calculated tendon excursions with Landmeer's first model, it is difficult to measure the required variables for this equation in living participants. The anthropometric regression model developed by Armstrong and Chaffin (1978) can be used to calculate FDP and FDS tendon excursions with limited inputs (joint thicknesses and posture). However, the regression equations are based on belt-pulley models, which assume constant radii of curvature. Keir and Wells (1999) showed that the radii are not constant when wrist and finger postures are manipulated with a magnetic resonance imaging technique.

Still researchers have used these models to estimate extrinsic wrist and finger flexor tendon excursions. Keir and Bach (2000) measured the distal fibre locations of the FDP and FDS muscle bellies and used the anthropometric regression equations to calculate tendon excursions with wrist extension. The researchers suggested that the muscle bellies have the potential to enter the carpal tunnel, which might be a mechanism for increased carpal tunnel pressure. Nelson et al. (2000) used lightweight optoelectric goniometers to measure finger posture during different typing conditions. These postures were used to calculate cumulative tendon excursions using the regression equations

developed by Chaffin and Armstrong (1978). Cumulative tendon excursions increased with different combinations of keyboard roll, pitch and yaw. More specifically, excursions were primarily affected by keyboard pitch. In a similar study, Treaster and Marras (2000) showed that cumulative tendon excursions during typing were dependent on gender even though they accounted for anthropometric variation. Sommerich et al. (1996) quantified wrist and finger postures with electrogoniometers during keyboarding. Subsequently, the researchers calculated tendon excursions with the anthropometric regression equations to estimate injury risk.

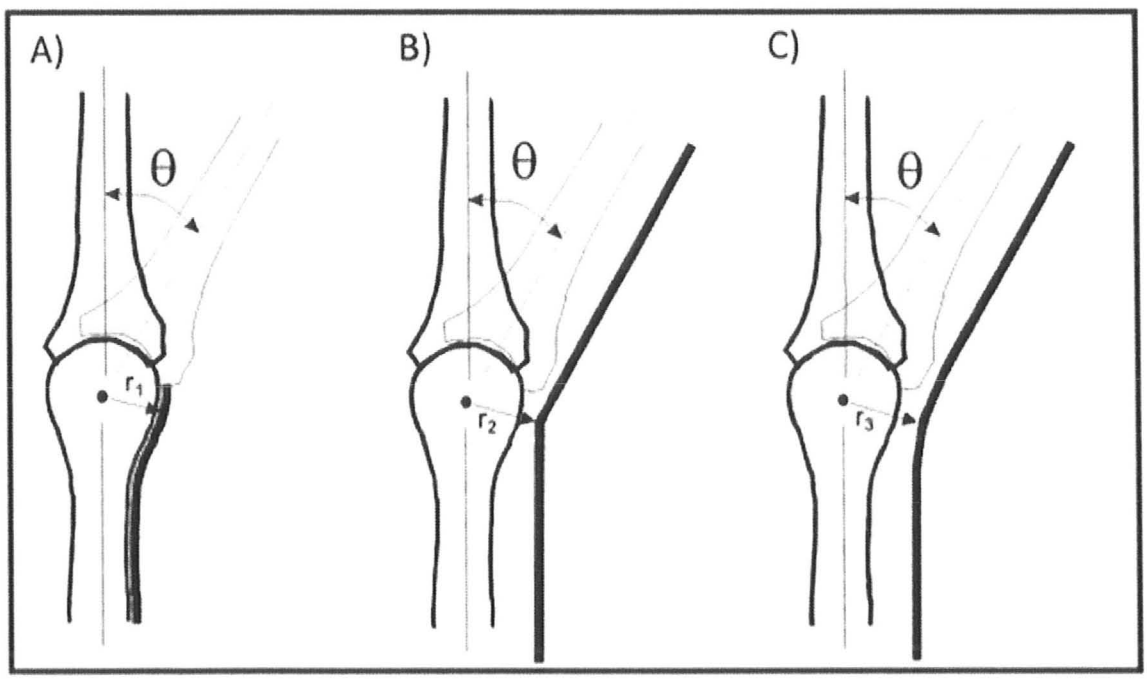

Figure 2.4. Landsmeer's tendon excursion models. A: In Landsmeer's model I, the tendon is on the curve of the proximal bone articular surface. B: In model II, the tendon is tethered at a single point. C: In model III, the tendon is curved with an annular pulley. From Keir et al., 1999 (page 637).

$$x = r\theta \quad (2.3)$$

where, x = tendon excursion (m);
r = distance from joint centre to tendon (m);
θ = joint displacement (rad).

$$x = 2r\sin(\theta/2), \quad (2.4)$$

where, x = tendon excursion (m);
r = distance from joint centre to geometric tendon constraint (m);
θ = joint displacement (rad).

$$x = 2y + \theta d - \theta y/\tan(\theta/2) \quad (2.5)$$

where, x = tendon excursion (m);
y= distance from joint centre to tendon (m);
d = distance form bone shaft to tendon (m);
θ = joint displacement (rad).

2.7. Lumbrical Muscle Incursions

Since the lumbricals originate from the FDP tendons, researchers have hypothesized that these muscles might be a mechanism for CTS. Cobb et al. (1994) found that the lumbricals moved into the carpal tunnel with increased wrist flexion. More specifically, the lumbricals moved 30 mm, on average, into the carpal tunnel with full wrist flexion. In a follow-up study, Cobb et al. (1995) measured carpal tunnel pressure with and without intact lumbricals in cadavers at different levels of finger flexion. Carpal tunnel pressure increased when the lumbricals were intact and did not change when they were removed with finger flexion (Cobb et al., 1995). Siegel et al.

(1995) also showed that the lumbrical origins were located more proximally in 128 patients undergoing carpal tunnel release compared to 40 healthy hand cadavers.

2.8. Biomechanical Models of the Hand and Fingers

Biomechanical models of the musculoskeletal system have great potential for studying injury mechanisms, improving tendon and nerve exercises during rehabilitation and directing surgical procedures. Several hand and finger models have been developed to study muscular coordination and joint loading in different work simulations (Wu et al., 2009; Mogk and Keir, 2007; Holzbaur et al., 2005; Li et al., 2000; Valero-Cuevas et al., 1998; Leijnse et al., 1993; 1992; An et al., 1979). An et al. (1979) developed a musculoskeletal hand model that incorporated average anatomical data from 10 cadaveric specimens. Joint kinematics and tendon paths were obtained from x-ray film. Modelled tendon locations were represented with line segments defined by two points at each joint. More recently, researchers developed a two-dimensional model capable of determining individual contributions of both the extrinsic and intrinsic finger flexors to finger joint moments (Li et al., 2000). Keir and Mogk (2007) developed a three-dimensional finger model using commercially available software (Maya™ 5.0, Alias®, Toronto, ON). The solid material mechanics inherent in this program allow for tissue interactions to be considered during force transmission. Early validations were limited to FDP and FDS tendon excursions with PIP and DIP flexion.

Even though several biomechanists have developed musculoskeletal hand models, they are rarely used by the scientific community (Delp and Loan, 1995). Researchers

have developed a computer software standard for representing musculoskeletal models (Delp et al., 2007; Delp and Loan, 1995). The commercially available Software for Interactive Musculoskeletal Modelling (SIMM) toolkit (MusculoGraphics Incorporated, Santa Rosa, CA) allows users to develop and distribute musculoskeletal models (Delp and Loan, 1995). More recently, an open-source software package called OpenSim was introduced to encourage further collaboration (Delp et al., 2007). These graphics-based modelling platforms allow the user to interact with complex musculoskeletal representations.

Musculoskeletal models in SIMM and OpenSim contain rigid body segments that are linked by joints (Delp and Loan, 1995). Each body segment has a reference frame that includes one or more bones (Delp and Loan, 1995). These segments are connected by the joint definitions, which include transformations and rotations that relate the relative locations of two bodies in three-dimensional space (Delp and Loan, 1995). Users can also program generalized coordinates to specify degrees of freedom such as joint angular displacement. More specifically, kinematic functions are used to describe translations and rotations with respect to generalized coordinates (Delp and Loan, 1995).

The geometry of musculotendon actuators in SIMM and OpenSim are specified by a series of points connected by lines (Delp and Loan, 1995). Each musculotendon control point is attached to the reference frame of an individual body segment (Delp and Loan, 1995). Musculotendon length is calculated as the sum of the individual lines that connect control points. The moment arms are computed using a partial velocity method,

which is advantageous since one consistent method can be used for many different types of joint configurations (Delp and Loan, 1995).

Musculotendon force in SIMM and OpenSim is calculated using a Hill-type model (Delp and Loan, 1995). The inputs for a musculotendon model include peak isometric force (F_o^M), optimal fibre length (L_o^M), tendon slack length (L_s^T) and pennation angle (α_o). These inputs are used to scale the active and passive force-length curves for muscles and passive force-length curve for tendon (Figure 2.5). The total force of a musculotendon actuator is the sum of the active and passive components (Zajac, 1989).

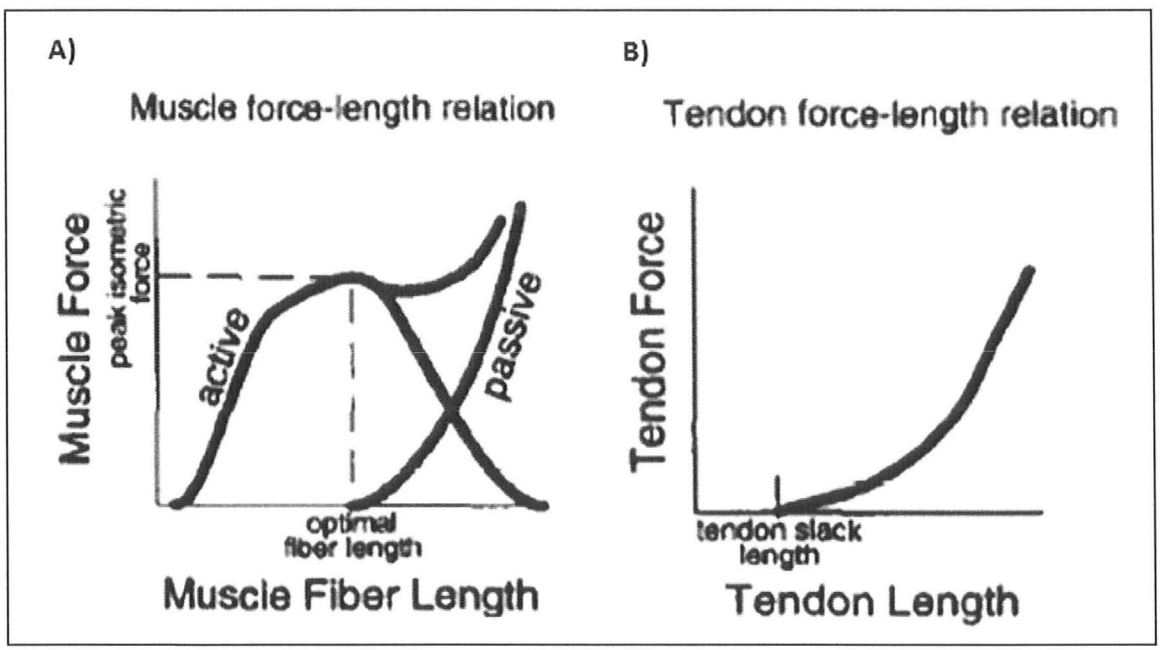

Figure 2.5. Muscle and tendon force-length relationships. A: Active and passive force-length curves for muscle. B: Passive force-length curve for tendon. From Delp and Loan, 1995 (page 24).

The anatomical characterises used to scale a Hill-type muscle model are important in determining its specific function (Lieber et al., 1997). The excursion of a musculotendon unit is the distance a muscle contracts added to the distance a muscle is stretched from its L_S^T (Fridén and Lieber, 2002). Musculotendon length is the mathematical sum of muscle length and tendon length once a correction factor for muscle pennation is applied (Garner and Pandy, 2003). If tendon is assumed to be infinitely stiff, for simplicity, then any musculotendon length change occurs at the muscle. When an actuator has both large maximum (L_{Mas}^{MT}) and minimum (L_{Min}^{MT}) lengths, then L_O^M is small and L_S^T is large (Figure 2.6a). When an actuator has large maximum and small minimum lengths, then L_O^M is large and L_S^T is small (Figure 2.6b). Consequently, L_O^M, L_S^T, L_{Mas}^{MT} and L_{Min}^{MT} are all important features that dictate muscle function.

A few researchers have measured the architectural design of forearm and hand muscles using cadaveric specimens. Lieber et al. (1992) measured muscle length and mass as well as fibre length and pennation angle for several muscles that span the wrist including the FDP and FDS. Sarcomere length was also measured with a laser diffraction method. Subsequently, physiological cross-sectional area and fibre length to muscle length ratios were computed. Other researchers have used similar methods to obtain extrinsic and intrinsic hand muscle architecture (Jacobson et al., 1992; Brand et al., 1981). While these studies contain relatively small samples, the datasets can be used to adjust Hill-type muscle model parameters when they are considered together. Still, subject-specific features, including physical (anthropometric) and functional (Hill-type model) parameters should be considered in order obtain accurate moment calculations

(Winby et al., 2008). SIMM and OpenSim can be used to perform anthropometric scaling. However, scaling L_O^M and L_S^T is more difficult (Winby et al., 2008). Several researchers have developed methods to estimate L_S^T with some success (Lee et al., 2008; Vilimek, 2006; Manal and Buchanan, 2004).

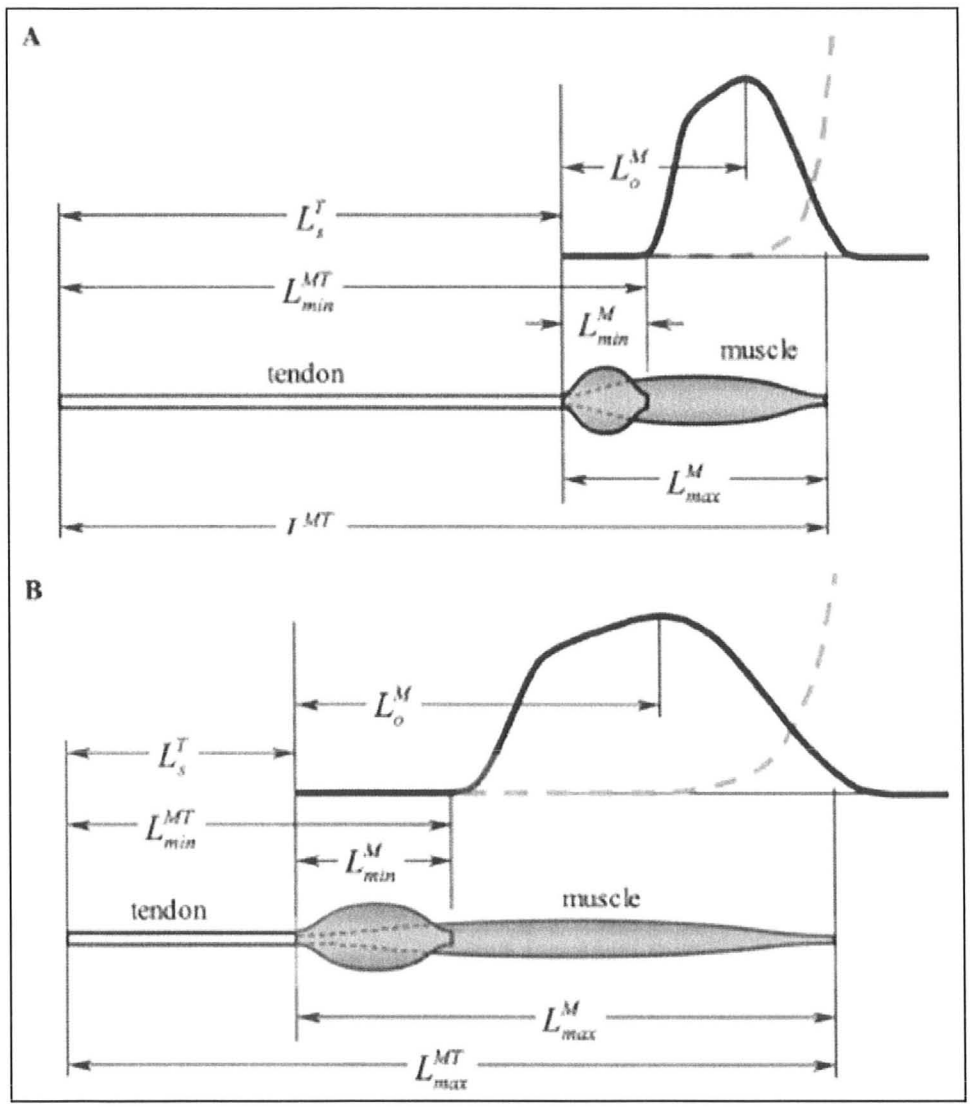

Figure 2.6. Relationship between optimal fibre length (L_O^M), tendon slack length (L_S^T) and maximum (L_{Mas}^{MT}) and minimum (L_{Min}^{MT}) musculotendon length. A: When L_S^T is large and L_O^M is small then excursion is small. B: When L_S^T is small and L_O^M is large then excursion is large. From Garner and Pandy, 2003 (page 209).

Although several musculoskeletal models exist for individual joints of the upper extremity, only one SIMM and OpenSim compatible model incorporates the shoulder, elbow, wrist, thumb and index finger (Holzbaur et al., 2005). The MCP linkage of the index finger was modelled as a universal joint to represent flexion/extension and abduction/adduction. The PIP and DIP linkages were modelled as hinges to represent flexion/extension. Since detailed descriptions of the finger joint rotation axes did not exist for the index finger, cylinders were fit at the bone surfaces to characterize movement. The extrinsic finger flexors and extensors for the index finger were modelled using data from a previous tendon excursion study (An et al., 1983). Hill-type muscle model parameters were also derived from experimental data (Jacobson et al., 1992; Lieber et al., 1992).

However, even this model is incomplete in several capacities. The MCP, PIP and DIP joints for the middle, ring and little fingers of the hand do not have programmed movement capabilities. As such, the model cannot be used in its present form to calculate these tendon excursions. Furthermore, the current anatomical model represents a 50^{th} percentile male. Modelling anthropometrical variation might also improve our current understanding of injury mechanisms since tendon excursions are dependent on finger anthropometry including joint thicknesses (An et al., 1979; Armstrong & Chaffin, 1978). Accordingly, efforts to model finger joint movement and realistic FDP and FDS excursions are needed to improve the usability of the current model for studying differential tendon motion.

2.9. Summary

The exact pathomechanics of many distal upper extremity WMSDs are not well understood. Differential motion between the FDP, FDS and MN likely contribute to the development of wrist and hand tendinopathies and CTS. A musculoskeletal model with realistic tendon excursions (and the potential to add a friction component) might be useful to further study WMSDs of the distal upper extremity. Holzbaur et al. (2005) recently developed a three-dimensional musculoskeletal model of the upper extremity for simulating surgery and analyzing neuromuscular control. However, several additions are needed to assess FDP and FDS tendon motion.

CHAPTER 3 - MANUSCRIPT

Modelling Extrinsic Finger Flexor Tendon Excursions and Moment Arms: Anatomic Fidelity vs. Function

Aaron M. Kociolek and Peter J. Keir*

Department of Kinesiology, McMaster University, Hamilton, Ontario, Canada

To be submitted to: *Journal of Biomechanics*

* Corresponding Author:
Peter J. Keir, PhD
Department of Kinesiology
McMaster University
1280 Main Street West
Hamilton, Ontario, L8S 4K1
Phone: (905) 525-9140 ext. 23543
Fax: (905) 523-6011
Email: pjkeir@mcmaster.ca

3.1. Abstract

A musculoskeletal model of the hand is needed to investigate the pathomechanics of tendon-related disorders and carpal tunnel syndrome. The purpose of this study was to develop a model with realistic extrinsic finger flexor tendon excursions and moment arms. An existing upper extremity model served as a starting point, which had programmed movement for the index finger. Movement capabilities were added to the middle, ring and little fingers. Metacarpophalangeal linkages were modelled as universal joints to simulate flexion/extension and abduction/adduction. Interphalangeal linkages were modelled as hinge joints to simulate flexion/extension. Extrinsic finger flexor tendon paths were modelled using two different approaches. The first method used control points fixed in the metacarpal and phalangeal coordinate systems to represent the annular and cruciate pulleys. The second method used wrapping surfaces at the metacarpophalangeal and interphalangeal joints to model constant moment arms with finger movement. Extrinsic finger flexor tendon excursions and moment arms in both the control point and joint wrapping models were iteratively adjusted to match the anthropometric regression model developed by Armstrong and Chaffin (1978) for a 50^{th} percentile male. Musculoskeletal scaling algorithms were also used to further evaluate the control point and joint wrapping models. More specifically, metacarpal and phalangeal segments were adjusted to determine the effects of length and thickness scaling on tendon kinematics. Tendon excursions and moment arms in the joint wrapping model best matched the anthropometric regression model. However, anatomical features of the tendons paths at the finger joints were not preserved in the joint wrapping model as

noted by ultrasound imaging. Depending on user needs, both anatomic fidelity and model outcomes should be considered as compromises may be necessary in the modelling process.

Keywords – Model; Hand; Finger; Tendon Excursion; WMSDs

3.2. Introduction

The exact pathomechanics of many distal upper extremity work-related musculoskeletal disorders (WMSDs) are not well understood. A common pathological finding in patients with wrist and hand tendinopathies and carpal tunnel syndrome (CTS) is non-inflammatory fibrosis and thickening of the synovium that surrounds the extrinsic finger flexor tendons (Barr et al., 2004). These histological observations are characteristic of degeneration due to repeated mechanical stress (Schuind et al., 1990). Also, pathological changes to the SSCT are most evident close to the tendons, which suggest that shear forces due to differential motion might be involved in distal upper extremity injury mechanisms (Armstrong et al., 1984). Researchers have also shown that fibrosis of the subsynovial connective tissue (SSCT) influence flexor digitorum profundus (FDP) and flexor digitorum superficialis (FDS) tendon gliding in the carpal tunnel (Ettema et al., 2008; 2007). In a recent study, it was found that cadavers with CTS had increased adherence or dissociation between the FDS tendons and SSCT compared to healthy controls (Ettema et al., 2008). These changes in tendon gliding might further increase frictional forces resulting in a viscous cycle of degradation (Ettema et al., 2006a; 2006b).

Differential motion between adjacent extrinsic finger flexor tendons, the median nerve and other carpal tunnel structures (such as carpal bones, bursae and the transverse carpal ligament) might also be involved in distal upper extremity injury mechanisms (Yoshii et al., 2008; Zhao et al., 2007). Recently, researchers measured gliding resistance of the middle finger FDS tendon in the carpal tunnel using healthy cadaveric specimens

(Zhao et al., 2007). Two movement conditions were tested (moving all fingers together and moving the middle finger alone) in different wrist flexion/extension postures. The highest peak and mean gliding resistances occurred with extreme wrist flexion while moving the middle finger alone. In another study, researchers developed a 2-dimensional model for calculating tendon frictional work (the product of displacement and shear force) as part of a method for quantifying injury risk (Moore et al., 1991). The researchers showed that frictional work estimates in the laboratory were highly correlated with upper extremity injury statistics in an epidemiology study by Silverstein et al. (1987) using similar task definitions to quantify force and frequency. A three-dimensional biomechanical model for investigating differential tendon motion and frictional work might be important in understanding injury mechanisms of flexor tendinitis, tenosynovitis and CTS.

Several researchers have measured extrinsic wrist and finger flexor tendon excursions *in vitro* (Ettema et al., 2008; 2007; Yamaguchi et al., 2008; Ugbolue et al., 2005; Netscher et al., 1998; 1997; Horii et al., 1993; 1992; Szabo et al., 1994; Minamikawa et al., 1992; An et al., 1983; Armstrong and Chaffin, 1978; Brand et al., 1975). Armstrong and Chaffin (1978) studied the effects of hand anthropometry on tendon excursion in healthy hand cadavers. The researchers developed linear regression equations to predict FDP and FDS excursions from joint thicknesses and posture, which were based on Landsmeer's (1960) geometrical tendon models. An et al. (1983) also found that tendon excursions were related to joint thicknesses in a cadaver study of the index finger. More recently, researchers have measured relative excursions of the

extrinsic finger flexor tendons and the median nerve in order to determine the effects of differential motion on wrist and hand disorders (Yamaguchi et al., 2008; Ugbolue et al., 2005).

Tendon excursions have also been measured *in vivo* using high-frequency ultrasound methods (Lopes, 2007; Oh et al., 2007; Erel et al., 2003; Dilley et al., 2001; Hough et al., 2000; Buyruk et al., 1998; Cigali et al., 1996). Lopes (2007) measured FDS tendon excursions in 16 healthy and 6 self-identified cumulative trauma disorder participants using spectral Doppler ultrasound. Tendon excursions calculated with the ultrasound method were larger compared to the regression model developed by Armstrong and Chaffin (1978). These discrepancies might be due to cadaveric measurement methods used in previous tendon excursion studies. Several other researchers have used colour Doppler imaging to measure extrinsic finger flexor tendon excursions (Erel et al., 2003; Hough et al., 2000; Cigali et al., 1996). Still, further research is required to validate tendon excursions using ultrasound methods.

Biomechanists and ergonomists have used tendon excursion models to study injury risks associated with different workplace tasks. Keir and Bach (2000) measured the distal fibres of the FDP and FDS muscle bellies. The anthropometric-based regression equations developed by Armstrong and Chaffin (1978) were used to calculate tendon excursions during wrist extension. The mean distances of the distal FDP and FDS muscle bellies from the pisiform were 4.9 and 9.3 mm, respectively. Both the FDP and FDS muscles had the potential to enter the carpal tunnel with extreme wrist extension. Researchers have also used tendon excursion models to predict injury risk during

keyboarding tasks due to differential tendon motion in the carpal tunnel (Nelson et al., 2000; Treaster and Marras, 2000; Sommerich et al., 1996).

While anthropometric-based methods are used to predict tendon excursions in ergonomic studies, there is a need to update this approach with current biomechanical modelling techniques. Biomechanical models of the musculoskeletal system have great potential for studying injury mechanisms of the distal upper extremity. Several models of the hand and fingers have been used to study muscular coordination and joint loading in workplace tasks (Wu et al., 2009; Mogk and Keir, 2007; Holzbaur et al., 2005; Li et al., 2000; Valero-Cuevas et al., 1998; Leijnse et al., 1993; 1992; An et al., 1979). Researchers have also developed a computer software standard for representing biomechanical models of the musculoskeletal system (Delp and Loan, 1995). The modelling platform (SIMM, MusculoGraphics Incorporated, Santa Rosa, CA) allows users to develop and distribute musculoskeletal models. An open-source program (OpenSim) for using musculoskeletal models is also available (Delp et al., 2007). Holzbaur et al. (2005) recently developed a SIMM and OpenSim compatible three-dimensional model of the upper extremity that simulates movement at the shoulder, elbow, forearm, wrist, thumb and index finger. However, movement capabilities of the middle, ring and little fingers with realistic FDP and FDS excursions are required in order to further study differential tendon motion.

The purposes of this study were to: 1) develop a biomechanical model with realistic extrinsic finger flexor tendon excursions and moment arms; 2) compare and contrast different modelling approaches to constrain tendon paths; 3) determine the

effects of anthropometrical scaling on tendon excursions and moment arms; 4) use high-frequency ultrasound to measure finger joint moment arms in three participants and compare these results with the current models.

3.3. Methods

Commercially available software (SIMM 4.1, MusculoGraphics Incorporated, Santa Rosa, CA) was used to model joint kinematics and musculotendon anatomy in the hand. A recently developed three-dimensional upper extremity model that represents movement at the shoulder, elbow, forearm, wrist, thumb and index finger served as a starting point (Holzbaur et al., 2005). This model has graphical representations of the hand bones, which are scaled to represent a 50^{th} percentile male (Holzbaur et al., 2005).

3.3.1. Joint Kinematics

Movement capabilities of the middle, ring and little fingers were added to the Holzbaur et al. (2005) model. Currently, there are no useable data that describes finger joint axes of rotation. Holzbaur et al. (2005) previously determined the axes of rotation for the index finger joints by fitting the long axes of cylinders to the articular surfaces of the metacarpals and phalanges. Neutral finger joint postures for the index finger were defined by aligning the long axes of the metacarpal and proximal, middle and distal phalanges. Even though the middle, ring and little fingers did not have programmed movement, metacarpal and phalangeal axes were also previously estimated to define articulations in neutral finger joint postures (Holzbaur et al., 2005). Metacarpophalangeal (MCP) linkages of the middle, ring and little fingers were modelled as universal joints (2

hinges at 90° to each other) with two degrees-of-freedom to simulate flexion/extension and abduction/adduction. Proximal and distal interphalangeal (DIP and PIP) linkages were modelled as hinges with one degree-of-freedom to simulate flexion/extension. Range of motion parameters were set to 50° extension - 90° flexion for the MCP joints and 0° - 90° flexion for the PIP and DIP joints, which are similar to those previously specified for the index finger (Holzbaur et al., 2005).

3.3.2. Muscle Paths

Eight extrinsic finger flexor musculotendon units were included in the Holzbaur et al. (2005) upper extremity model, which were the FDP and FDS for the index (i), middle (m), ring (r) and little (l) fingers. Since the Holzbaur et al. (2005) model had limited movement capabilities at the hand, only the FDPi and FDSi were originally adjusted to best match tendon excursions and moment arms from experimental data (An et al., 1983). In the current study, two different modelling approaches were used to manually adjust the tendon paths of the extrinsic finger flexors for all the fingers. In both approaches, anatomical constraints were iteratively adjusted to best match tendon excursions and moment arms for a 50^{th} percentile male using the anthropometric-based regression equations developed by Armstrong and Chaffin (1978).

The first approach involved using control points fixed in bone local coordinate systems. The tendon paths were defined by line segments connecting adjacent control points. The control points constrained the tendon paths at the bone surfaces in a similar manner to annular and cruciate pulleys in the fingers. More specifically, the control points constrained the tendon paths close to the palmar surfaces of the metacarpals and

phalanges. The control points also prevented extreme bowstringing of the tendons at the finger joints with movement. However, not every annular and cruciate pulley was represented with a fixed point. While this model did preserve some anatomical characteristics of the finger flexor tendon paths, the control points were adjusted to obtain realistic tendon excursions and moment arms during the modelling process. Wrapping objects were also used at the finger joints to prevent the tendons from passing through bone at extreme joint angles. This approach was called the control point (CP) method (Figure 3.1a). The second modelling approach involved using wrappings at the finger joints as anatomical constraints. More specifically, tendons were fixed to the surfaces of elliptical (for the MCP joints) and cylindrical (for the PIP and DIP joints) wrap objects at the finger joints, which resulted in relatively constant moment arms with movement. Control points were also used between the wrap objects to fix the FDP and FDS paths at the MCP, PIP and DIP joints and prevent tendon excursion and moment arm interactions with complex finger movements. This approach was termed the joint wrapping (JW) method (Figure 3.1b).

****

Figure 3.1

****

3.3.3. Muscle Architecture

Force-generating capacities of the FDP and FDS units were previously specified in the original upper extremity model since these muscles are important actuators of the wrist joint (Holzbaur et al., 2005). Muscle architecture was represented using a Hill-type model, which requires four parameters to scale force. These parameters are peak isometric force (F_o^M), optimal fibre length (L_o^M), pennation angle (α_o) and tendon slack length (L_s^T). Holzbaur et al. (2005) obtained F_o^M, L_o^M, and α_o from muscle architecture studies to represent force generating capabilities for a 50th percentile male (Jacobson et al., 1992; Lieber et al., 1992). Since L_s^T is not described in these studies, inputs were originally selected for the finger flexors to match active and passive wrist moment measurements for human subjects (Holzbaur et al., 2005). However, musculotendon paths of the FDP and FDS were changed in the current CP and JW models. Accordingly, L_s^T were adjusted to preserve the original force generating capabilities of the FDP and FDS. More specifically, L_s^T were corrected for the changes in musculotendon lengths of the FDP and FDS, which shifted the muscle and tendon force-length relationships to the original operating ranges at the wrist joint. Subsequently, maximum isometric force and moment generating capabilities of the FDP and FDS with MCP, PIP and DIP flexion/extension in both the CP and JW models were calculated to evaluate function.

3.3.4. Anthropometrical Scaling

Musculoskeletal scaling methods were applied to the index finger of Holzbaur et al. (2005) model and the current CP and JW models. More specifically, bone lengths, thicknesses and combined lengths and thicknesses were scaled to represent 10th, 25th,

50^{th}, 75^{th} and 90^{th} percentile anthropometrics. Scaling factors were calculated from anthropometric hand studies where segment lengths and joint thicknesses were measured (Greiner, 1991; Garrett, 1970). The manual scaling toolset in OpenSim was used to apply scaling factors in the x, y and z bone axes. Muscle control points attached to the bone coordinate systems were also scaled by this procedure. However, muscle wrapping objects did not adjust with the OpenSim scaling toolset. The wrap objects in the scaled models were manually adjusted with SIMM. Subsequently, tendon excursions and moment arms in the scaled models were compared to the regression models of Armstrong and Chaffin (1978).

3.3.5. Experimental Evaluation of Modelled Moment Arms

Hand anthropometry and moment arms were measured in 3 right hand dominant participants (2 males and 1 female) to further evaluate the current CP and JW models. The participants were selected so that significant anthropometric variations in finger dimensions (including metacarpal and phalangeal segment lengths and joint thicknesses) were observed.

3.3.5.1. Hand Measurements

Finger dimensions were measured with calipers according to previous anthropometric studies of the hand (Greiner, 1991; Garrett, 1970). The measurements included metacarpal and proximal, middle and distal phalange lengths and MCP, PIP and DIP joint thicknesses of the index, middle, ring and little fingers. Furthermore, descriptive statistics (population means and standard deviations) in hand anthropometry studies were used in order to calculate z-scores for the collected finger dimensions.

These scores were used to obtain percentile ratings from the z-table (Greiner, 1991; Garrett, 1970).

3.3.5.2. Ultrasound Imaging

Grey-scale sonography was used to obtain DICOM images of extrinsic finger flexor tendons at the MCP, PIP and DIP joints. Each participants was comfortably seated with their forearm supinated and elbow flexed at approximately 120° on an adjustable surface. The ultrasound scans were performed with a 7.5 MHz linear array probe (model SSH-140A, Toshiba, Tochigi-Ken, Japan) on the palmar side of the hand in a neutral posture. All scanning procedures were completed in the sagittal plane.

Moment arms of the FDP and FDS were calculated from the DICOM images using the ruler tool in Adobe Photoshop 10.0 (Adobe Systems Inc., San Jose, CA). A calibration factor (pixels-to-mm) embedded in the image header was used to appropriately adjust the ruler tool. Joint rotation centres were estimated by fitting the curves of ellipses to the proximal bone heads at each joint (Schneck and Bronzino, 2003). Moment arms were measured at the smallest perpendicular distances between the estimated joint centres and the FDP and FDS tendons.

3.3.6. Analysis

Pearson's correlations were used to test the linearity of modelled tendon excursions with finger joint flexion/extension. Subsequently, mean FDP and FDS tendon excursions per 100° of MCP, PIP and DIP flexion/extension were calculated. Since the CP and JW models are representative of an average male, tendon excursions were compared to the regression model of Armstrong and Chaffin (1978) using 50^{th} percentile

anthropometrics. Mean, minimum and maximum FDP and FDS moment arms were also calculated through MCP, PIP and DIP flexion/extension and compared to the regression model for a 50th percentile male. Mean and peak root mean squared differences (RMSD) between the CP and JW models and the regression model for both tendon excursions and moment arms were also reported to further evaluate the current approaches. The effects of anatomical scaling on tendon excursions and moment arms in the CP and JW hand models were also compared to the anthropometric regression model.

Experimental moment arms (calculated from ultrasound images) were compared to the current musculoskeletal hand models. Stepwise linear regression analyses were also used to determine if relationships existed between externally measured hand anthropometrics (including metacarpal and phalangeal segment lengths and joint thicknesses) and internally measured FDP and FDS moment arms at the finger joints in neutral posture.

3.4. Results

3.4.1. Tendon Excursions

3.4.1.1. CP Model

Extrinsic finger flexor tendon excursions in the CP hand model demonstrated linear relationships ($r > 0.98$) with MCP, PIP and DIP flexion/extension of the index finger (Figure 3.2). Generally, tendon excursions of the FDPi and FDSi were similar to the regression model developed by Armstrong and Chaffin (1978) for a 50th percentile male (Table 3.1). Mean RMSD were small, ranging from 0.15 mm (FDPi with DIP

flexion/extension) to 0.72 mm (FDSi with MCP flexion/extension). However, peak RMSD for the FDPi and FDSi at 50° MCP extension were 2.23 mm and 2.66 mm, respectively (Appendix A).

Tendon excursions for the middle, ring, and little fingers had similar relationships. Extrinsic finger flexor tendon excursions were linear ($r > 0.98$) with MCP, PIP and DIP flexion/extension. Generally, tendon excursions were similar to the Armstrong and Chaffin (1978) regression model. However, FDP and FDS tendon excursions with MCP extension were smaller than predicted by the anthropometric regression equations.

****

Figure 3.2

****

3.4.1.2. JW Model

Tendon excursions of the FDPi and FDSi were linear ($r > 0.99$) with MCP, PIP and DIP flexion/extension of the index finger. Generally, excursions in the JW hand model best matched Armstrong and Chaffin (1978) for a 50th percentile male (compared to the CP model). Mean RMSDs were between 0.10 mm (FDPi with DIP flexion/extension) and 0.63 mm (FDSi with MCP flexion/extension). Peak RMSDs for the FDPi and FDSi tendon excursions with MCP flexion/extension were 1.45 mm and 1.39 mm, respectively. These peak differences occurred at 90° MCP flexion. Results for excursions of the middle, ring, and little fingers were similar. Tendon excursions of the

FDP and FDS were linear with MCP, PIP and DIP flexion/extension. Generally, tendon excursions in the JW model best matched Armstrong and Chaffin (1978) for a 50th percentile male (compared to the CP model).

****

Table 3.1

****

3.4.2. Moment Arms

3.4.2.1. CP Model

Mean FDPi and FDSi moment arms in the CP model were similar compared to anthropometric regression for a 50th percentile male (Table 3.2). However, moment arms at the MCP and PIP joints were variable with flexion/extension. As a result, minimum and maximum values in the CP hand model differed from the constant moment arms calculated by Armstrong and Chaffin (1978). The largest mean RMSD were for MCP moment arms, which were 1.70 mm and 1.91 mm in the FDPi and FDSi, respectively. Peak RMSD for MCP moment arms were 3.19 and 3.73 mm in the FDPi and FDSi, respectively. Moment arms results were similar for the middle, ring and little fingers.

3.4.2.2. JW Model

Extrinsic finger flexor moment arms in the JW hand model were similar to Armstrong and Chaffin (1978) for a 50th percentile male. Moment arms in the JW model were relatively constant throughout finger joint ranges of motion (compared to the CP

model). Consequently, mean, minimum and maximum moment arms at MCP, PIP and DIP joints best matched the anthropometric regression model. The largest mean RMSD were for MCP moment arms, which were 0.78 mm and 0.80 mm in the FDPi and FDSi, respectively. Peak RMSDs for MCP moment arms were 1.34 mm and 1.35 mm in the FDPi and FDSi, respectively. Moment arms for the middle, ring and little fingers in the JW model also best matched Armstrong and Chaffin (1978) for a 50^{th} percentile male (compared to the CP model).

****

Table 3.2

****

3.4.3. Anthropometric Scaling

Anatomical scaling of the index finger had an effect on extrinsic finger flexor tendon excursions and moment arms in both the CP and JW models. In the CP model, FDPi and FDSi tendon excursions with PIP flexion were sensitive to bone length and thickness scaling (Appendix B). Similarly, moment arms at the PIP joint were sensitive to bone length scaling in early joint flexion and bone thickness scaling in late joint flexion (Figure 3.3). In the JW model, FDPi and FDSi tendon excursions and moment arms with PIP flexion were sensitive to bone thickness scaling only. Furthermore, anatomical scaling of the JW model had similar effects on tendon excursion and moment

arms compared to the regression model developed by Armstrong and Chaffin (1978). However, the effect of joint thickness scaling on tendon excursions and moment arms were more sensitive than predicted by the regression model.

****

Figure 3.3

****

3.4.4. Evaluation of Modelled Moment Arms with Ultrasound

Average joint thickness measurements of the index finger were 25.0 ± 4.4 mm, 17.3 ± 2.1 mm and 13.0 ± 1.7 mm at the MCP, PIP and DIP joints, respectively (Table 3.3). Moment arms of the FDPi were 8.4 ± 1.1 mm (MCP), 9.6 ± 0.8 mm (PIP) and 6.4 ± 1.2 mm (DIP). Similarly, FDSi moment arms were 10.0 ± 0.9 mm and 8.3 ± 0.6 mm for the MCP and PIP joints, respectively (Table 3.4). Generally, experimentally measured moment arms of the PIP joint were similar to the JW model in a neutral posture. However, experimental moment arms of the index finger were smaller at the MCP joint and larger at the DIP joint compared to the JW hand model. Similar findings were also observed for the middle, ring and little fingers (Appendix C).

Linear regression showed that FDP and FDS moment arms of the finger joints were related to each MCP, PIP and DIP joint thicknesses (Appendix D). The coefficients of determination at the MCP joint were 0.663 for the FDP and 0.743 for the FDS. The highest coefficients of determination were at the PIP joint, which were 0.883 for the FDP

and 0.939 for the FDS. The coefficient of determination at the DIP joint was 0.661 for the FDP.

****

Tables 3.3 and 3.4

****

3.5. Discussion

The purpose of this study was to develop a SIMM and OpenSim compatible musculoskeletal model of the hand for calculating extrinsic finger flexor tendon excursions. A biomechanical model with realistic FDP and FDS excursions would be useful for studying differential tendon motion in workplace tasks to ultimately predict frictional forces and the risk of developing a musculoskeletal disorder. Also, anatomical scaling algorithms in OpenSim could be used in these studies to represent participant-specific anthropometric variation. In the current study, two models with different extrinsic finger flexor tendon paths were developed. The control point (CP) model defined tendon paths with a series of points connected by line segments. The control points constrained the tendon paths at the palmar surfaces of the metacarpals and phalanges in the hand, similar to annular and cruciate pulleys. Consequently, the control points preserved some anatomical features of the extrinsic finger flexor tendon paths. The JW hand model used the contours of wrap objects to define the tendon paths at the finger joints and maintain relatively constant moment arms. While this approach

constrained the finger flexors at the MCP, PIP and DIP joints, modelled tendon trajectories were not anatomically realistic.

The effects of scaling on extrinsic finger flexor tendon excursions and moment arms were evaluated to determine whether anthropometric variability could be included in biomechanical studies and improve modelling outcomes. In the CP hand model, FDP and FDS tendon excursions and moment arms with PIP flexion were influenced by length and thickness scaling of the phalanges. Even relatively small scaling adjustments of the control points (to represent 10^{th}, 25^{th}, 75^{th} and 90^{th} percentile hand anthropometry) resulted in large changes to tendon excursions and moment arms, especially at the extreme range of PIP flexion. For example, using anatomical scaling procedures to represent 75^{th} and 90^{th} percentile phalange lengths increased bowstringing of the finger flexors, which also dramatically increased both tendon excursions and moment arms with PIP flexion. When scaling was applied to the index finger of the Holzbaur et al. (2005) model, similar changes in FDP and FDS tendon excursion and moment arms occurred with PIP flexion. However, the anthropometric regression model developed by Armstrong and Chaffin (1978) demonstrated that tendon excursions and moment arms were dependent on joint thicknesses (but not segment lengths). Even though there were efforts to model realistic anatomical features of the extrinsic finger flexors in the CP model, anthropometrical scaling algorithms did not realistically change tendon excursions and moment arms.

In the JW hand model, FDP and FDS tendon excursions and moment arms with PIP flexion were only influenced by thickness scaling of the phalanges. This result is

similar to the anthropometric models developed by Armstrong and Chaffin (1978). However, scaling joint thicknesses in the index finger resulted in relatively large changes to tendon excursions and moment arms. The effects of anatomical scaling algorithms should be considered before applying them to pre-existing musculoskeletal models. Relatively small scaling adjustments can result in large changes to modelling outcomes, which was especially true for conventional modelling methods where musculotendon actuators are anatomically constrained by control points.

While the effects of scaling phalangeal lengths and thicknesses on tendon excursions and moment arms were successfully determined for the CP and JW models, representing anthropometric variability in OpenSim was a meticulous process. The scaling algorithm in OpenSim was not applied to the modelled wrap objects. Manual adjustments to the MCP, PIP and DIP joint wrapping surfaces were modelled in SIMM to represent anthropometric variability, which was a time consuming process. In a SIMM compatible model, a single musculotendon actuator can interact with several wrap objects to preserve different anatomical features. Efforts to include scaling algorithms for wrap objects in SIMM and OpenSim might allow researchers to realistically model anthropometric variability while reducing the time required these adjustments.

In the effort to evaluate anatomic fidelity, external and internal hand dimensions were also measured in three participants. Linear regressions showed that joint thickness measurements were related to FDP and FDS moment arms calculated from high-frequency ultrasound images. This finding is consistent with cadaver studies where moment arms were derived from experimental measurements of tendon excursions (An et

al., 1983; Armstrong and Chaffin, 1978). These data suggest that using anthropometrical-based scaling algorithms can be used to adjust internal modelling outcomes including tendon excursion and moment arms. However, moment arms obtained from ultrasound images were not always similar to the CP and JW hand models. The measured MCP moment arms were much smaller than the CP and JW models. Additional research is required to measures moment arms in different hand postures using MRI. This study could be used to further evaluate the CP and JW hand models and provide data for additional adjustments of the extrinsic finger flexors.

Biomechanical models of the musculoskeletal system that represent average anthropometrical data are frequently used in ergonomic studies. In this study, finger flexor paths were iteratively adjusted to match tendon excursion and moment arms for a 50^{th} percentile male. Tendon excursions in the CP hand model were typically similar to the regression model developed by Armstrong and Chaffin (1978) for a 50^{th} percentile male. However, tendon excursions with MCP extension were relatively small compared to the regression model. Incongruities in FDP and FDS moment arms with MCP flexion/extension were also evident due to the interaction between control points and the wrap objects. More specifically, moment arm incongruities in the CP model occurred since the FDP and FDS were fixed to wrap surfaces in MCP extension (so that the tendons did not pass through bones) but not in MCP flexion. Furthermore, extrinsic finger flexor moment arms varied with different finger joint postures. Discrepancies in model outcomes generally occurred because the control points did not realistically constrain tendon paths with extreme finger joint flexion resulting in bowstringing of the

tendon. While adding control points could function as further anatomical constraints, the tendon paths would become twisted when transformations and rotations were applied to the phalangeal local coordinate systems during finger joint movement. Despite attempts to preserve anatomic fidelity in the CP model, FDP and FDS tendon excursions and moment arms at the finger joints were not anatomically realistic.

The joint wrapping (JW) model involved using the contours of three-dimensional shapes (such as cylinders and ellipses) to fix the moment arms of FDP and FDS at the finger joints. The approach best matched both tendon excursions and moment arms described by Armstrong and Chaffin (1978) for a 50^{th} percentile male. However, the wrap objects resulted in circular tendon paths away from the bone surfaces. Consequently, the JW hand model did not preserve the anatomic fidelity of the annular and cruciate pulley systems. Based on these findings, it appears that trade-offs may exist between preserving the anatomic fidelity of the musculoskeletal system and modelling kinematic and kinetic outputs. Depending on user needs, both anatomic fidelity and model outcomes should be considered as compromises may be necessary in the modelling process.

Several investigators have measured FDP and FDS tendon excursions with different finger postures. However, research conducted by Armstrong and Chaffin (1978) represents the only study that tested all the fingers joints in the hand. The researchers also determined the effects of hand anthropometrics on tendon excursions in a series of regression equations. Even though these anthropometric models are extensively used in biomechanics and ergonomics studies, they are based on a limited sample of 4

hand cadavers. An et al. (1983) also measured finger flexor tendon excursions in the index finger of seven cadaveric specimens. While the researchers also demonstrated that a relationship existed between tendon excursions and joint thicknesses, relatively small female hand cadavers were tested. Consequently, tendon excursions were smaller than the JW model as well as the cadaver study by Armstrong and Chaffin (1978).

In a recent study, FDS tendon excursions of the index finger were determined using spectral Doppler ultrasound (Lopes, 2007). Tendon excursions with 90° MCP flexion were similar to both the CP and JW models as well as the regression model developed by Armstrong and Chaffin (1978). However, tendon excursions were not always linear in the ultrasound study. Furthermore, complex finger movements (such as full finger flexion) resulted in larger tendon excursions compared to the CP and JW models and the regression model. These data suggest that there may be an interaction effect with concurrent MCP, PIP and DIP finger flexion. However, further research is needed to validate the *in vivo* measurement methods using spectral Doppler ultrasound. Still, these preliminary results present a challenge for modelling extrinsic finger flexors since the tendon excursions in the current musculoskeletal models are fixed at each finger joint regardless of the other joints.

The main objectives of this study were to evaluate tendon excursions with the CP and JW modelling approaches. However, the Hill-type parameters of the extrinsic finger flexors were also adjusted for future studies involving force and moment generating capabilities. More specifically, the tendon slack lengths were adjusted to account for changes in musculotendon lengths of the FDP and FDS in the CP and JW models.

Subsequently, maximum isometric forces and moments were evaluated with different finger joint postures (Appendix E). Extrinsic finger flexor forces with MCP, PIP and DIP flexion in the CP and JW model were similar since the tendon excursions were alike. However, FDP and FDS forces with MCP and PIP flexion in the CP and JW models were different compared to the Holzbaur et al. (2005) upper extremity model. This result was expected since tendon excursions of the index finger were considerably smaller in the Holzbaur et al. (2005) model (compared to both the CP and JW models), which produced different force-length relationships. Moments at the index finger joints differed between the CP and JW models, which resulted primarily from differences in the modelled moment arms (since isometric forces were similar).

3.5.1. Limitations

There are a few limitations to the current musculoskeletal models. Tendon excursions and moment arms were tested for MCP, PIP and DIP joint flexion/extension using regression models for a 50^{th} percentile male. However, the anthropometric regression equations developed by Armstrong and Chaffin (1978) are only are based on a limited sample of 4 cadavers. Additional research using *in vivo* ultrasound methods with simple and complex finger movements is needed to evaluate tendon excursions in these models. Furthermore, FDP and FDS excursions and moment arms in the MCP abduction/adduction plane were not rigorously tested in the current models. The MCP abduction/adduction tendon excursions in the CP and JW models were larger than the cadaver measurements by An et al. (1983). However, these excursions were only tested in a few small female hand cadavers. Also, simple anatomically derived joint axes of

rotation were used in the CP and JW musculoskeletal models. Currently there are no available data that describes instantaneous centres of rotation for the finger joints. Incorporating these data in musculoskeletal models of the fingers might improve modelling outcomes while preserving anatomical fidelity.

3.5.2. Conclusions

The control point modelling approach used points in the phalangeal coordinate systems to represent anatomically realistic musculotendon paths, but produced moment arms that were not necessarily representative. The joint wrapping model involved using wrap objects at the finger joints as anatomical constraints and while best matching previous data did not preserve anatomic fidelity of the tendon paths at the finger joints. Anatomical scaling of the hand models also showed that the joint wrapping approach best matched tendon excursions and moment arms compared to the anthropometric regression models. Depending on user needs, both anatomic fidelity and model outcomes should be considered as compromises may be necessary in the modelling process. The current joint wrapping (fixed moment arm) model represents a useful research tool for studying differential tendon motion of the extrinsic finger flexor tendons.

3.6. References

An, K. N., Chao, E.Y., Cooney, W.P. and Linscheid, R.L. 1979. Normative model of human hand for biomechanical analysis. *Journal of Biomechanics* 12, 775-788.

An, K.N., Ueba, Y., Chao, E.Y., Cooney, W.P. and Linscheid, R.L. 1983. Tendon excursion and moment arm of index finger muscles. *Journal of Biomechanics* 16 (6), 419-425.

Armstrong, T.J. and Chaffin, D.B. 1978. An investigation of the relationship between displacements of the finger and wrist joints and the extrinsic finger flexor tendons. *Journal of Biomechanics* 11, 119-128.

Armstrong, T.J., Castelli, W.A., Evans, G. and Diaz-Perez, R. 1984. Some histological changes in carpal tunnel contents and their biomechanical implications. *Journal of Occupational Medicine* 26 (3), 197-201.

Barr, A.E., Barbe, M.F. and Clark, B.D. 2004. Work-related musculoskeletal disorders of the hand and wrist: epidemiology, pathophysiology, and sensorimotor changes. *Journal of Orthopaedic and Sports Physical Therapy* 34 (10), 610-627.

Brand, P.W., Cranor, K.C. and Ellis, J.C. 1975. Tendon and pulleys at the metacarpophalangeal joint of a finger. *The Journal of Bone and Joint Surgery* 57, 779-784.

Buyruk, H.M., Holland, W.P.J., Snijders, C.J., Laméris, J.S., Hoorn, E., Stoeckart, R. and Stam, H.J. 1998. Tendon excursion measurements with colour Doppler imaging. *Journal of Hand Surgery* 23B (3), 350-353.

Cigali, B.S., Buyruk, H.M., Snijders, C.J., Lameris, J.S., Holland, W.P.J., Mesut, R. and Stam, H.J. 1996. Measurement of tendon excursion velocity with colour Doppler imaging: a preliminary study on flexor pollicus longus muscle. *European Journal of Radiology* 23 217-221.

Delp, S.L., Anderson, F.C., Arnold, A.S., Loan, P., Habib, A., John, C.T., Guendelman, E. and Thelen, D.G. 2007. OpenSim: open-source software to create and analyze dynamic simulations of movement. *Transactions on Biomedical Engineering* 54 (11), 1940-1948.

Delp, S.L. and Loan, J.P. 1995. A graphics-based software system to develop and analyze models of musculoskeletal structures. *Computers in Biology and Medicine* 25 (1), 21-34.

Dilley, A., Greening, J., Lynn, B., Leary, R. and Morris, V. 2001. The use of cross-correlation analysis between high-frequency ultrasound images to measure longitudinal median nerve movement. *Ultrasound in Medicine and Biology* 27 (9), 1211-1218.

Erel, E., Dilley, A., Greening, J., Morris, V., Cohen, B. and Lynn, B. 2003. Longitudinal sliding of the median nerve in patients with carpal tunnel syndrome. *Journal of Hand Surgery* 28B (5), 439-443.

Ettema, A.M., Amadio, P.C., Zhao, C., Wold, L.E., O'Byrne, M.M., Moran, S.L. and An, K.N. 2006a. Changes in the functional structure of the tenosynovium in idiopathic carpal tunnel syndrome: a scanning electron microscope study. *Plastic and Reconstructive Surgery* 118 (6), 1413-1422.

Ettema, A.M., An, K.N., Zhao, C., O'Byrne, M.M. and Amadio, P.C. 2008. Flexor tendon and synovial gliding during simultaneous and single digit flexion in idiopathic carpal tunnel syndrome. *Journal of Biomechanics* 41, 292-298.

Ettema, A.M., Belohlavek, M., Zhao, C., Oh, S.H., Amadio, P.C. and An, K.N. 2006b. High-resolution ultrasound analysis of subsynovial connective tissue in human cadaver carpal tunnel. *Journal of Orthopaedic Research* 24, 2011-2020.

Ettema, A.M., Zhao, C., Amadio, P.C., O'Byrne, M.M. and An, K.N. 2007. Gliding characteristics of flexor tendon and tenosynovium in carpal tunnel syndrome: a pilot study. *Clinical Anatomy* 20, 292-299.

Greiner, T.M. 1991. Hand anthropometry of U.S. army personnel. Document AD-A244 533. Natick, MA. United States Natick Research, Development and Engineering Center.

Holzbaur, K.R.S., Murray, W.M. and Delp, S.L. 2005. A model of the upper extremity for simulating musculoskeletal surgery and analyzing neuromuscular control. *Annals of Biomedical Engineering* 33 (6), 829-840.

Horii, E., An, K.N. and Linscheid, R.L. 1993. Excursion of prime wrist tendons. *Journal of Hand Surgery* 18A, 83-90.

Horii, E., Lin, G.T., Cooney, W.P., Linscheid, R.L. and An, K.N. 1992. Comparative flexor tendon excursion after passive mobilization: an in vitro study. *Journal of Hand Surgery* 17A, 559-566.

Hough, A.D., Moore, A.P. and Jones, M.P. 2000. Peripheral nerve motion measurement with spectral doppler sonography: a reliability study. *Journal of Hand Surgery* 25B (6). 585-589.

Jacobson, M.D., Raab, R., Fazeli, B.M., Abrams, R.A., Batte, M.J. and Lieber, R.L. 1992. Architectural designs of the hand muscles. *Journal of Hand Surgery* 17A, 804-809.

Keir, P.J. and Bach, J.M. 2000. Flexor muscle incursion into the carpal tunnel: a mechanism for increased carpal tunnel pressure? *Clinical Biomechanics* 15 (5), 301-305.

Landsmeer, J.M.F. 1960. Studies in the anatomy of articulation. *Acta Morph. Neerlands Scand*, 3-4.

Leijnse, J.N.A.L., Bonte, J.E., Landsmeer, J.M.F., Kalker, J.J., Van Der Meulen, J.C. and Snijders, C.J. 1992. Biomechanics of the finger with anatomical restrictions – the significance for the exercising hand of the musician. *Journal of Biomechanics* 25 (11), 1253-1264.

Leijnse, J.N.A.L., Snijders, C.J., Bonte, J.E., Landsmeer, J.M.F., Kalker, J.J., Van Der Meulen, J.C., Sonneveld, G.J. and Hovius, S.E.R. 1993. The hand of the musician: the kinematics of the bidigital finger system with anatomical restrictions. *Journal of Biomechanics* 26 (10), 1169-1179.

Li, Z.M., Zatsiorsky, V.M. and Latash, M.L. 2000. Contribution of the extrinsic and intrinsic hand muscles to the moments in finger joints. *Clinical Biomechanics* 15, 103-211.

Lieber, R.L., Jacobson, M.D., Fazeli, B.M., Abrams, R.A. and Botte, M.J. 1992. Architecture of selected muscles of the arm and forearm: anatomy and implications for tendon transfer. *Journal of Hand Surgery* 17A (3), 787-798.

Lopes, M. M. 2007. *Ultrasound measures of the carpal tunnel, tendon and nerve excursion*. Thesis (M.Sc.). York University.

Minamikawa, Y., Peimer, C.A., Yamaguchi, T., Banasiak, N.A., Kambe, K. and Sherwin, F.S. 1992. Wrist positions and extension tendon amplitude following repair. *Journal of Hand Surgery* 17A, 268-271.

Mogk, J.P.M. and Keir, P.J. 2007. Modelling extrinsic finger flexor tendon kinematics. Proceedings of 29th Annual Meeting of the American Society of Biomechanics, Cleveland, Ohio.

Moore, A., Wells, R. and Ranney, D. 1991. Quantifying exposure in occupational manual tasks with cumulative trauma disorder potential. *Journal of Ergonomics* 34 (12), 1433-1453.

Nelson, J.E., Treaster, D.E. and Marras, W.S. 2000. Finger motion, wrist motion and tendon travel as a function of keyboard angles. *Clinical Biomechanics* 15, 489-498.

Netscher, D., Dinh, T., Cohen, V. and Thornby, J. 1998. Division of the transverse carpal ligament and flexor tendon excursion: open and endoscopic carpal tunnel release. *Plastic and Reconstructive Surgery* 102 (3), 773-778.

Netscher, D., Mosharrafa, A., Lee, M., Polsen, C., Choi, H., Steadman, A.K. and Thornby, J. 1997. Transverse carpal ligament: its effect on flexor tendon excursion, morphologic changes of the carpal canal, and on pinch and grip strengths after open carpal tunnel release. *Plastic and Reconstructive Surgery* 100 (3), 636-642.

Oh, S., Belohlavek, M., Zhao, C., Osamura, N., Zobitz, M.E. and An, K. 2007. Detection of differential gliding characteristics of the flexor digitorum superficialis tendon and subsynovial connective tissue using color Doppler sonographic imaging. *Journal of Ultrasound Medicine* 26, 149-155.

Schneck, D.J. and Bronzino, J.D. 2003. Biomechanics: Principles and Applications. First Edition. CRC Press. New York, NY.

Schuind, F., Ventura, M. and Pasteels, J.L. 1990. Idiopathic carpal tunnel syndrome: histologic study of the flexor synovium. *Journal of Hand Surgery* 15A: 497-503.

Sommerich, C.M., Marras, W.S. and Parnianpour, M. 1996. A quantitative description of typing biomechanics. *Journal of Occupational Rehabilitation* 6 (1), 33-55.

Szabo, R.M., Bay, B.K., Sharkey, N.A. and Gaut, C. 1994. Median nerve displacement through the carpal tunnel. *Journal of Hand Surgery* 19A, 901-906.

Treaster, D.E. and Marras, W.S. 2000. An assessment of alternate keyboards using finger motion, wrist motion and tendon travel. *Clinical Biomechanics* 15, 499-503.

Ugbolue, U.C., Hsu, W., Goitz, R.J. and Zong-Ming, L. 2005. Tendon and nerve displacement at the wrist during finger movements. *Clinical Biomechanics* 20, 50-56.

Valero-Cuevas, F.J., Zajac, F.E. and Burgar, C.G. 1998. Larger index fingertip forces are produced by subject-independent patterns of muscle excitation. *Journal of Biomechanics* 31, 693-703.

Wu, J.Z., An, K.N., Cutlip, R.G., Andrew, M.E. and Dong, R.G. 2009. Modeling of the muscle/tendon excursions and moment arms in the thumb using the commercial software anybody. *Journal of Biomechanics* 42, 383-388.

Yamaguchi, T., Osamura, N., Zhao, C., An, K.N. and Amadio, P.C. 2008. Relative longitudinal motion of the finger flexors, subsynovial connective tissue, and median nerve before and after carpal tunnel release in a human cadaver model. *Journal of Hand Surgery* 33A, 888-892.

Yoshii, Y., Zhao, C., Henderson, J., Zhao, K.D., Zobitz, M.E., An, K.N. and Amadio, P.C. 2008. Effects of carpal tunnel release on the relative motion of the tendon, nerve, and subsynovial connective tissue in a human cadaver model. *Clinical Biomechanics* 23, 1121-1127.

Zhao, C., Ettema, A.M., Osamura, N., Berglund, L.J., An, K.N and Amadio, P.C. 2007. Gliding characteristics between flexor tendons and surrounding tissues in the carpal tunnel: a biomechanical cadaver study. *Journal of Orthopaedic Research* 25, 185-190.

3.7. Manuscript Tables and Figures

Table 3.1. Extrinsic finger flexor tendon excursions with MCP, PIP and DIP flexion/extension (mm/100°).

		Index Finger			Middle Finger			Ring Finger			Little Finger		
		MCP	PIP	DIP	MCP	PIP	DIP	MCP	PIP	DIP	MCP	PIP	DIP
FDP	CP	21.1	17.9	8.3	21.4	19.1	8.8	19.6	18.1	8.3	17.7	17.7	7.6
	JW	23.3	16.9	8.8	23.9	17.7	8.9	21.1	17.1	8.5	19.5	15.3	7.7
	A&C	22.2	17.5	8.4	22.6	17.8	8.6	21.7	17.3	8.3	20.3	16.4	7.7
FDS	CP	22.3	16.2	-	22.7	16.9	-	21.3	15.9	-	19.5	15.2	-
	JW	24.9	15.2	-	25.1	16.1	-	22.8	15.3	-	20.8	13.9	-
	A&C	23.8	15.5	-	24.2	15.8	-	23.4	15.3	-	21.9	14.3	-

Table 3.2. Extrinsic finger flexor moment arms with MCP, PIP and DIP flexion/extension (mm).

			Index Finger			Middle Finger			Ring Finger			Little Finger		
			MCP	PIP	DIP	MCP	PIP	DIP	MCP	PIP	DIP	MCP	PIP	DIP
FDP	CP	Average	12.1	10.2	4.7	12.3	10.9	5.0	11.2	10.4	4.7	10.2	10.1	4.3
		Minimum	9.5	7.4	4.3	8.3	7.5	4.1	9.2	7.1	4.2	8.4	6.6	4.0
		Maximum	14.6	11.7	5.0	14.9	12.6	5.3	13.4	12.3	5.3	12.3	11.9	4.7
	JW	Average	13.4	9.7	5.0	13.5	10.1	5.2	12.1	9.8	4.9	11.1	8.8	4.4
		Minimum	11.9	9.3	4.7	11.8	9.8	4.8	10.3	9.3	4.4	9.5	8.5	4.2
		Maximum	14.1	9.9	5.2	14.3	10.3	5.8	12.8	10.0	5.2	12.2	8.9	4.5
	A&C		12.7	10.0	4.8	12.9	10.2	5.0	12.5	9.9	4.7	11.6	9.4	4.4
FDS	CP	Average	12.7	9.2	-	13.2	9.7	-	12.2	9.1	-	11.2	8.7	-
		Minimum	9.9	6.4	-	8.7	6.4	-	9.8	5.8	-	8.8	5.0	-
		Maximum	15.5	10.8	-	15.6	11.4	-	14.7	11.3	-	13.9	10.9	-
	JW	Average	14.3	8.7	-	14.5	9.2	-	13.1	8.8	-	11.9	7.9	-
		Minimum	12.3	8.2	-	12.9	8.8	-	11.3	8.2	-	9.9	7.7	-
		Maximum	15.0	8.9	-	15.3	9.4	-	13.8	9.0	-	13.0	8.1	-
	A&C		13.6	8.9	-	13.9	9.0	-	13.4	8.7	-	12.6	8.2	-

Table 3.4. Moment arms of the index finger (mm).

			Index Finger		
Participant	**Sex**	**Tendon**	**MCP**	**PIP**	**DIP**
1	**M**	**FDP**	9.3	10.0	7.3
		FDS	11.0	8.7	-
2	**F**	**FDP**	7.7	8.9	5.6
		FDS	9.3	7.5	-
3	**M**	**FDP**	8.1	9.8	6.4
		FDS	9.8	8.5	-
Average (SD)		**FDP**	**8.4 (1.1)**	**9.6 (0.8)**	**6.4 (1.2)**
		FDS	**10.0 (0.9)**	**8.3 (0.6)**	**-**

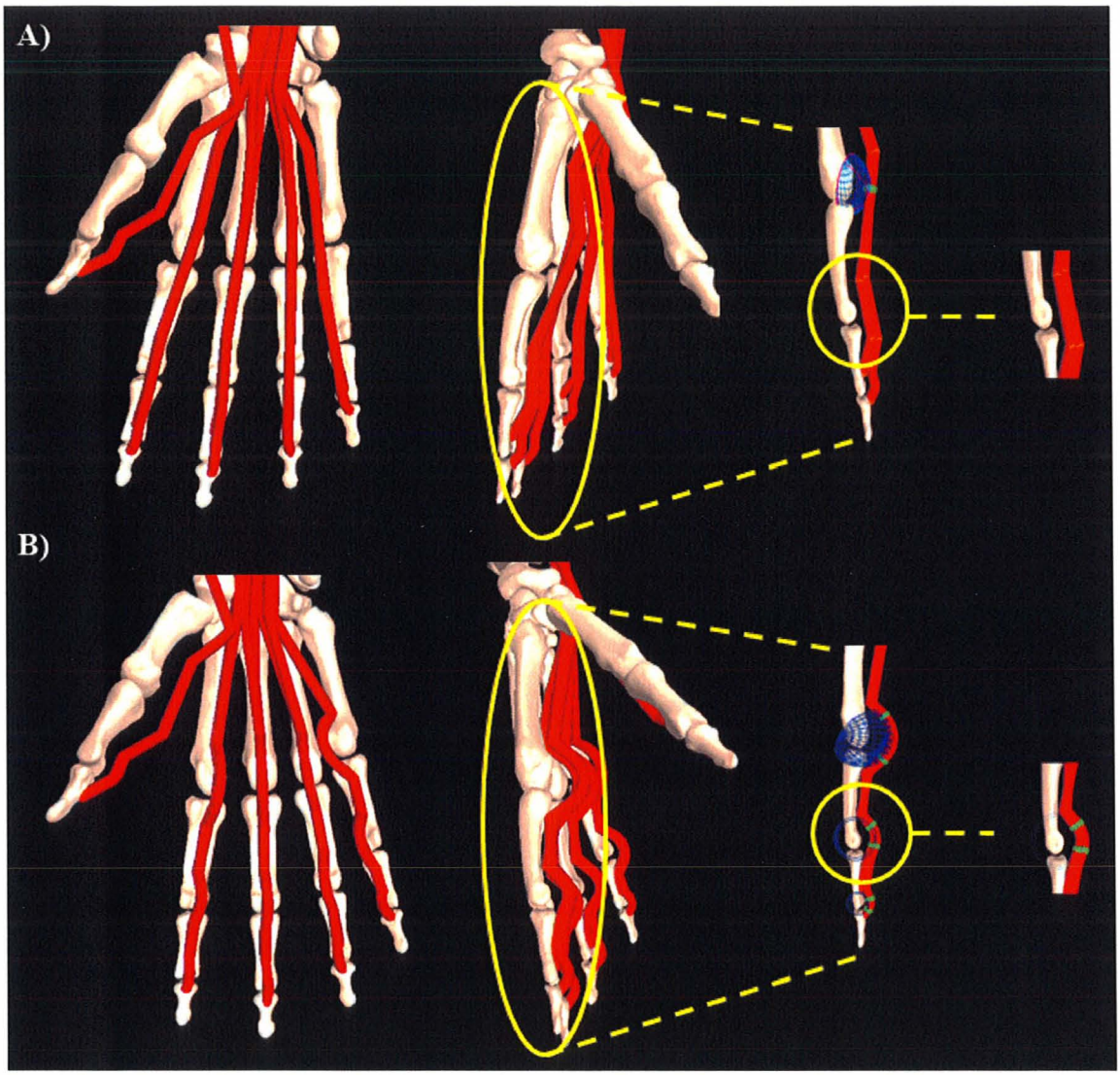

Figure 3.1. Palmar (up) and sagittal (down) views of the (a) CP and (b) JW models illustrating musculotendon geometry (red cords), control points (orange) and wrap objects (blue).

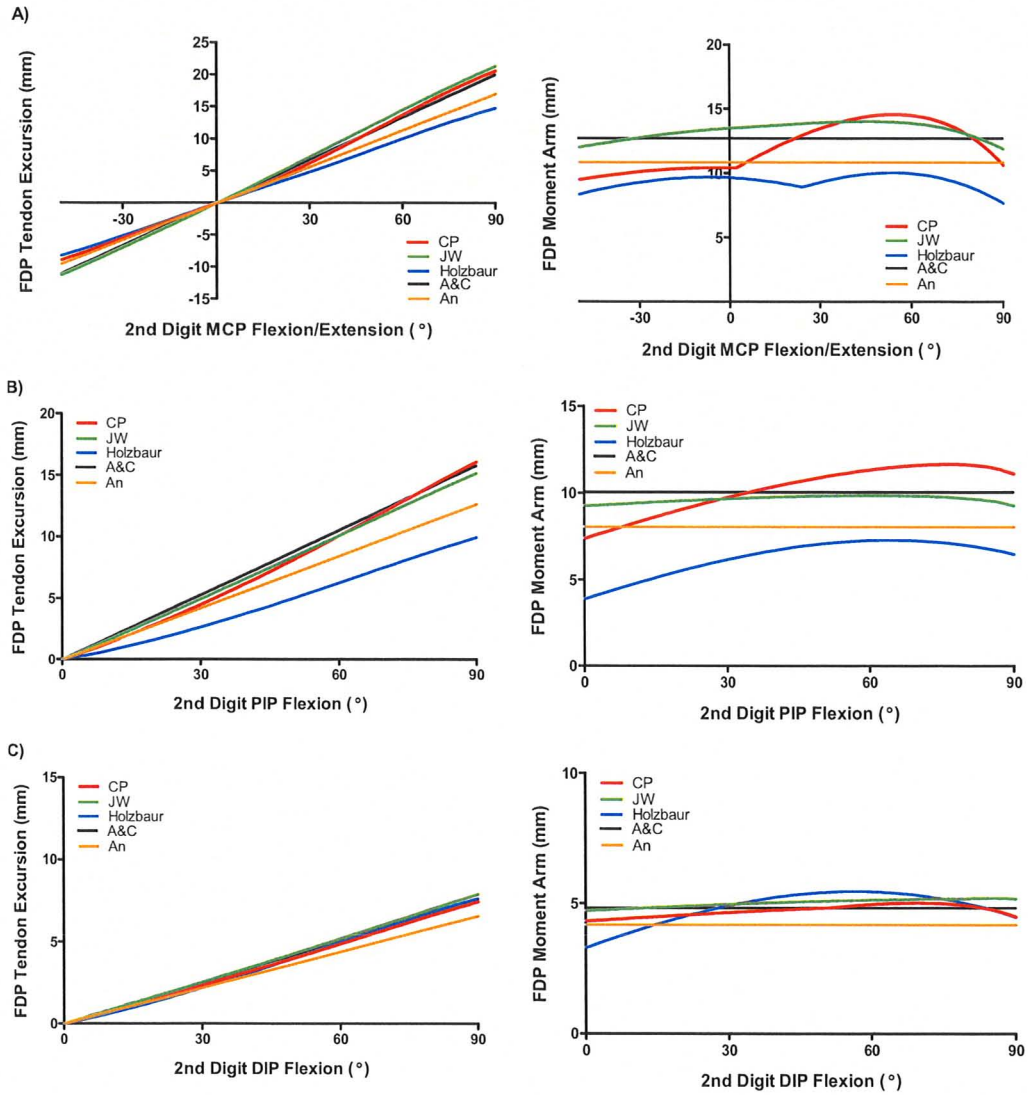

Figure 3.2. FDP tendon excursions (left) and moment arms (right) with index finger (a) MCP, (b) PIP and (c) DIP flexion. CP – Control point model; JW – Joint wrapping model; Holzbaur – Holzbaur et al. (2005) upper extremity model; A&C – Armstrong and Chaffin (1978) regression model ; An – An et al., (1983) experimental data.

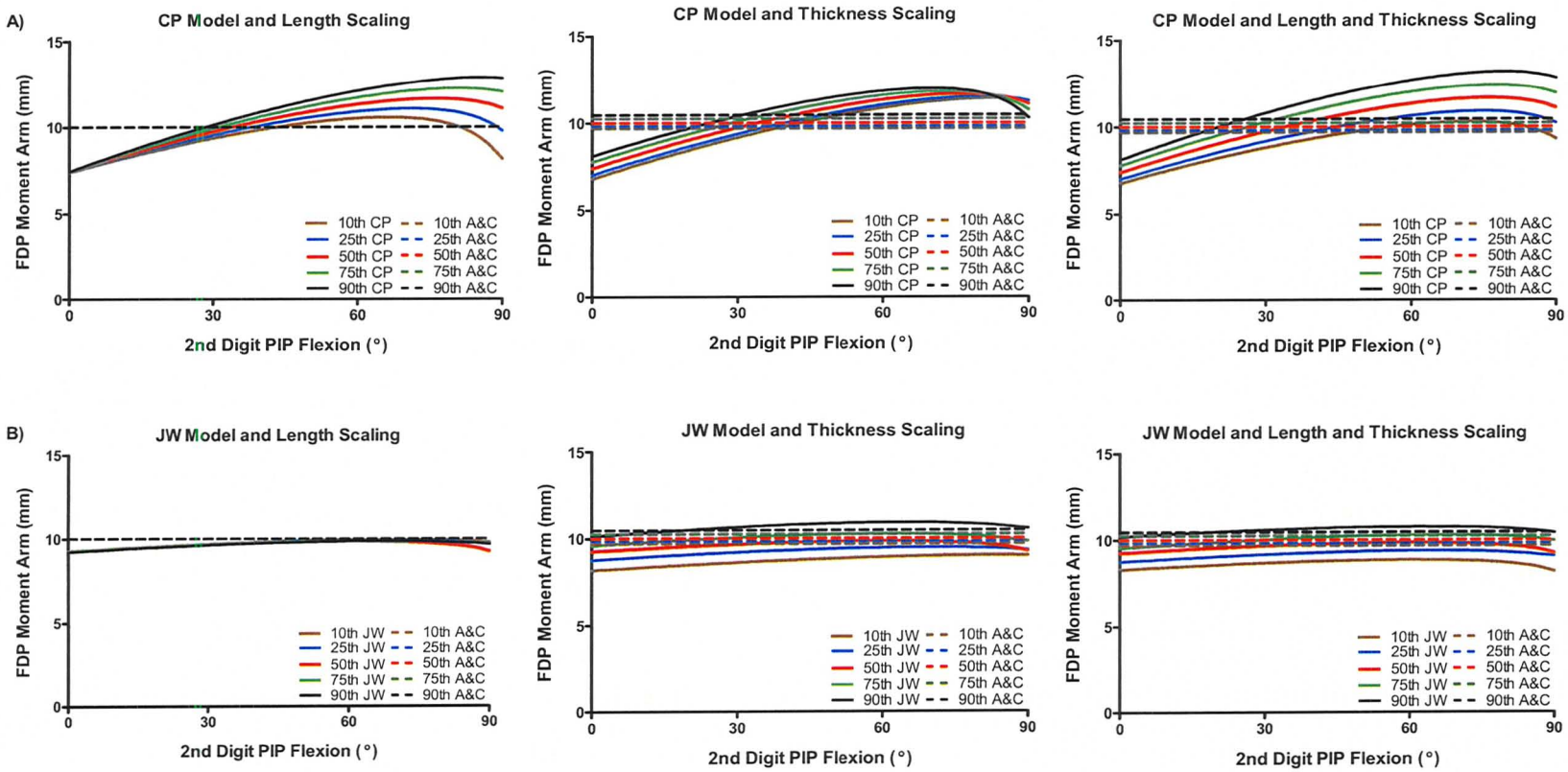

Figure 3.3. FDPi moment arms with phalangeal length scaling (left), thickness scaling (centre) and length and thickness scaling (right). CP – Control point model; JW – Joint wrapping model; A&C – Armstrong and Chaffin (1978) regression model. Anthropometrical scaling corresponds to dimensions for 10th, 25th, 50th, 75th and 90th percentile males.

CHAPTER 4 - THESIS SUMMARY AND FUTURE DIRECTIONS

The mechanisms for many WMSDs of the distal upper extremity remain uncertain. Recently, researchers have suggested that differential motion between the extrinsic finger flexors might contribute in the development of flexor tendinitis, tenosynovitis and CTS. A detailed biomechanical hand model would be useful for studying differential tendon motion in workplace tasks to ultimately predict frictional forces and the risk of developing a WMSD. This study represents a first effort towards developing a model with realistic FDP and FDS tendon excursions. In the current study, two different musculoskeletal models were developed. These models had movement capabilities at the index, middle, ring and little fingers. The control point (CP) model used points fixed in the phalangeal coordinate systems to constrain the extrinsic finger flexor tendons in the fingers. The joint wrapping (JW) model used wrap objects at the finger joints to fix the tendon paths. Tendon excursions and moment arms in the JW hand model best matched Armstrong and Chaffin (1978) for a 50^{th} percentile even though the tendon paths were not anatomically correct. The ability to represent anatomical characteristics of the musculoskeletal system and obtain realistic outcomes (including tendon excursions and moment arms) appear to be somewhat limited by the current modelling methods. Still, the JW model can be used to investigate differential tendon motion in different work tasks.

Additional research is required to measure tendon excursions and moment arms *in vivo* using diagnostic imaging equipment (including ultrasound and MRI) to further

validate the current musculoskeletal hand model as well as revisit the anthropometric-based regression models developed by Armstrong and Chaffin (1978). In a recent ultrasound study, Lopes (2007) showed that tendon excursions of the index finger were larger than predicted by the regression model during complex finger movements. However, further validations are required for dynamic measurements of the finger flexor tendons. Measuring FDP and FDS tendon excursions *in vivo* might also improve current understanding of injury mechanisms and assist in future modelling studies. Furthermore, cadaver studies that quantify friction in the carpal tunnel with different postures, forces and work cycles are necessary for better understanding injury mechanisms. Efforts to integrate frictional estimates with tendon excursion models of the hand are needed to further study distal upper extremity WMSDs. The current musculoskeletal models represent a first step in developing a friction model of the finger flexor tendons.

Several additions to the current hand models are also needed. Currently, the intrinsic hand muscles are not included in the model. Modelling the intrinsic muscles presents a challenge since their origins and insertions are complex and variable. The lumbricals originate from the deep finger flexor tendons. Consequently, the origins of the lumbricals move into the carpal tunnel with the FDP tendons during finger flexion. Also, the palmar and dorsal interossei have complex insertions into the extensor expansion. Despite these challenges, including intrinsic hand muscles would allow users to control the model using electromyography-assisted optimization methods. As such, the addition of hand intrinsics might assist in further studying injury mechanisms of flexor tendinitis, tenosynovitis and CTS.

REFERENCES

Amadio, P.C. 2005. Friction of the gliding surface: implications for tendon surgery and rehabilitation. *Journal of Hand Therapy* 18 (2), 112-119.

An, K. N., Chao, E.Y., Cooney, W.P. and Linscheid, R.L. 1979. Normative model of human hand for biomechanical analysis. *Journal of Biomechanics* 12, 775-788.

An, K.N., Ueba, Y., Chao, E.Y., Cooney, W.P. and Linscheid, R.L. 1983. Tendon excursion and moment arm of index finger muscles. *Journal of Biomechanics* 16 (6), 419-425.

Armstrong, T.J. and Chaffin, D.B. 1978. An investigation of the relationship between displacements of the finger and wrist joints and the extrinsic finger flexor tendons. *Journal of Biomechanics* 11, 119-128.

Armstrong, T.J., Fine, L.J., Goldstein, S.A., Lifshitz, Y.R. and Silverstein, B.A. 1987. Ergonomic considerations in hand and wrist tendinitis. *Journal of Hand Surgery* 12A (5), 830–837.

Armstrong, T.J., Castelli, W.A., Evans, G. and Diaz-Perez, R. 1984. Some histological changes in carpal tunnel contents and their biomechanical implications. *Journal of Occupational Medicine* 26 (3), 197-201.

Barr, A.E., Barbe, M.F. and Clark, B.D. 2004. Work-related musculoskeletal disorders of the hand and wrist: epidemiology, pathophysiology, and sensorimotor changes. *Journal of Orthopaedic and Sports Physical Therapy* 34 (10), 610-627.

Beekman, R., Visser, L.H. 2003. Sonography in the diagnosis of carpal tunnel syndrome: a critical review of the literature. *Muscle and Nerve* 27, 26-33.

Brand, P.W. and Hollister, A. 1985. Clinical Mechanics of the Hand. 3rd Edition. CV Mosby. St. Louis, MO.

Brand, P.W., Beach, R.B. and Thompson, D.E. 1981. Relative tension and potential excursion of muscles in the forearm and hand. *Journal of Hand Surgery* 6A (3), 209-219.

Brand, P.W., Cranor, K.C. and Ellis, J.C. 1975. Tendon and pulleys at the metacarpophalangeal joint of a finger. *Journal of Bone and Joint Surgery* 57, 779-784.

Buyruk, H.M., Holland, W.P.J., Snijders, C.J., Laméris, J.S., Hoorn, E., Stoeckart, R. and Stam, H.J. 1998. Tendon excursion measurements with colour Doppler imaging. *Journal of Hand Surgery* 23B (3), 350-353.

Chao, E.Y., An, K.N., Cooney, W.P. and Linscheid, R.L. 1989. Biomechanics of the hand: a basic research study. 1st Edition. World Scientific. Teaneck, NJ.

Cigali, B.S., Buyruk, H.M., Snijders, C.J., Lameris, J.S., Holland, W.P.J., Mesut, R. and Stam, H.J. 1996. Measurement of tendon excursion velocity with colour Doppler imaging: a preliminary study on flexor pollicus longus muscle. *European Journal of Radiology* 23 217-221.

Cobb, T.K., An, K.N. and Cooney, W.P. 1995. Effect of lumbrical muscle incursion within the carpal tunnel on carpal tunnel pressure: a cadaveric study. *Journal of Hand Surgery* 20A (2), 186-192.

Cobb, T.K., Cooney, W.P. and Berger, R.A. 1994. Lumbrical muscle incursion into the carpal tunnel during finger flexion. *Journal of Hand Surgery* 19B (4), 434-438.

de Krom, M.C.T., Kester, A.D.M., Knipschild, P.G. and Spaans, F. 1990. Risk factors for carpal tunnel syndrome. *American Journal of Epidemiology* 132 (6), 1102–1110.

Delp, S.L., Anderson, F.C., Arnold, A.S., Loan, P., Habib, A., John, C.T., Guendelman, E. and Thelen, D.G. 2007. OpenSim: open-source software to create and analyze dynamic simulations of movement. *Transactions on Biomedical Engineering* 54 (11), 1940-1948.

Delp, S.L. and Loan, J.P. 1995. A graphics-based software system to develop and analyze models of musculoskeletal structures. *Computers in Biology and Medicine* 25 (1), 21-34.

Dilley, A., Greening, J., Lynn, B., Leary, R. and Morris, V. 2001. The use of cross-correlation analysis between high-frequency ultrasound images to measure longitudinal median nerve movement. *Ultrasound in Medicine and Biology* 27 (9), 1211-1218.

Eladoumikdachi, F., Valkov, P.L., Thomas, J. and Netscher, D.T. 2002a. Anatomy of the intrinsic hand muscles revisited: part I. interossei. *Journal of Plastic and Reconstructive Surgery* 110, 1211-1224.

Eladoumikdachi, F., Valkov, P.L., Thomas, J. and Netscher, D.T. 2002b. Anatomy of the intrinsic hand muscles revisited: part II. lumbricals. *Journal of Plastic and Reconstructive Surgery* 110, 1225-1231.

Erel, E., Dilley, A., Greening, J., Morris, V., Cohen, B. and Lynn, B. 2003. Longitudinal sliding of the median nerve in patients with carpal tunnel syndrome. *Journal of Hand Surgery* 28B (5), 439-443.

Ettema, A.M., Amadio, P.C., Zhao, C., Wold, L.E. and An, K.N. 2004. A histological and immunohistochemical study of the subsynovial connective tissue in idiopathic carpal tunnel syndrome. *Journal of Bone and Joint Surgery* 86, 1458–1466.

Ettema, A.M., Amadio, P.C., Zhao, C., Wold, L.E., O'Byrne, M.M., Moran, S.L. and An, K.N. 2006a. Changes in the functional structure of the tenosynovium in idiopathic carpal tunnel syndrome: a scanning electron microscope study. *Plastic and Reconstructive Surgery* 118 (6), 1413-1422.

Ettema, A.M., An, K.N., Zhao, C., O'Byrne, M.M. and Amadio, P.C. 2008. Flexor tendon and synovial gliding during simultaneous and single digit flexion in idiopathic carpal tunnel syndrome. *Journal of Biomechanics* 41, 292-298.

Ettema, A.M., Belohlavek, M., Zhao, C., Oh, S.H., Amadio, P.C. and An, K.N. 2006b. High-resolution ultrasound analysis of subsynovial connective tissue in human cadaver carpal tunnel. *Journal of Orthopaedic Research* 24, 2011-2020.

Ettema, A.M., Zhao, C., Amadio, P.C., O'Byrne, M.M. and An, K.N. 2007. Gliding characteristics of flexor tendon and tenosynovium in carpal tunnel syndrome: a pilot study. *Clinical Anatomy* 20, 292-299.

Fridén, J. and Lieber, R. 2002. Mechanical considerations in the design of surgical reconstructive procedures. *Journal of Biomechanics* 35, 1039-1045.

Garner, B.A. and Pandy, M.G. 2003. Estimation of musculotendon properties in the human upper limb. *Annals of Biomedical Engineering* 31, 207-220.

Gerr, F., Marcus, M., Ensor, C., Kleinbaum, D., Cohen, S., Edwards, A., Gentry, E., Ortiz, D.J. and Monteilh, C. 2002. A prospective study of computer users: I. study design and incidence of musculoskeletal symptoms and disorders. *American Journal of Industrial Medicine* 41 (4), 221-235.

Greiner, T.M. 1991. Hand anthropometry of U.S. army personnel. Document AD-A244 533. Natick, MA. United States Natick Research, Development and Engineering Center.

Goodman, H.J. and Choueka, J. 2005. Biomechanics of the flexor tendons. *Hand Clinics* 21, 129-149.

Holzbaur, K.R.S., Murray, W.M. and Delp, S.L. 2005. A model of the upper extremity for simulating musculoskeletal surgery and analyzing neuromuscular control. *Annals of Biomedical Engineering* 33 (6), 829-840.

Horii, E., An, K.N. and Linscheid, R.L. 1993. Excursion of prime wrist tendons. *Journal of Hand Surgery* 18A, 83-90.

Horii, E., Lin, G.T., Cooney, W.P., Linscheid, R.L. and An, K.N. 1992. Comparative flexor tendon excursion after passive mobilization: an in vitro study. *Journal of Hand Surgery* 17A, 559-566.

Hough, A.D., Moore, A.P. and Jones, M.P. 2000. Peripheral nerve motion measurement with spectral doppler sonography: a reliability study. *Journal of Hand Surgery* 25B (6). 585-589.

Jacobson, M.D., Raab, R., Fazeli, B.M., Abrams, R.A., Batte, M.J. and Lieber, R.L. 1992. Architectural designs of the hand muscles. *Journal of Hand Surgery* 17A, 804-809.

Keir, P.J. and Bach, J.M. 2000. Flexor muscle incursion into the carpal tunnel: a mechanism for increased carpal tunnel pressure? *Clinical Biomechanics* 15 (5), 301-305.

Keir, P.J., Bach, J.M. and Rempel, D.M. 1998. Fingertip loading and carpal tunnel pressure: differences between a pinching and a pressing task. *Journal of Orthopaedic Research* 16 (1), 112-115.

Keir, P.J. and Wells, R.P. 1999. Changes in geometry of the finger flexor tendons in the carpal tunnel with wrist posture and tendon load: an MRI study on normal wrists. *Clinical Biomechanics* 14, 365-345.

Keir, P.J., Wells, R.P., Ranney, D.A. and Lavery, W. 1997. The effects of tendon load and posture on carpal tunnel pressure. *Journal of Hand Surgery* 22A, 628-634.

Keyserling, W.M. 2000. Workplace risk factors and occupational musculoskeletal disorders, part 2: a review of biomechanical and psychophysical research on risk factors associated with upper extremity disorders. *American Industrial Hygiene Association Journal* 61, 231-243.

Khan, M.K., Cook, J.L., Bonar, F., Harcourt, P. and Astrom, M. 1999. Histopathology of common tendinopathies update and implications for clinical management. *Sports Medicine* 27 (6), 393-408.

Landsmeer, J.M.F. 1960. Studies in the anatomy of articulation. *Acta Morph. Neerlands Scand*, 3-4.

Lee, W.E., Uhm, H.W. and Nam, Y.S. 2008. Estimation of tendon slack length of knee extension/flexion muscle. Proceedings of the International Conference on Control, Automation and Systems, Seoul, Korea.

Leijnse, J.N.A.L., Bonte, J.E., Landsmeer, J.M.F., Kalker, J.J., Van Der Meulen, J.C. and Snijders, C.J. 1992. Biomechanics of the finger with anatomical restrictions – the significance for the exercising hand of the musician. *Journal of Biomechanics* 25 (11), 1253-1264.

Leijnse, J.N.A.L., Snijders, C.J., Bonte, J.E., Landsmeer, J.M.F., Kalker, J.J., Van Der Meulen, J.C., Sonneveld, G.J. and Hovius, S.E.R. 1993. The hand of the musician:

the kinematics of the bidigital finger system with anatomical restrictions. *Journal of Biomechanics* 26 (10), 1169-1179.

Li, Z.M., Zatsiorsky, V.M and Latash, M.L. 2000. Contribution of the extrinsic and intrinsic hand muscles to the moments in finger joints. *Clinical Biomechanics* 15, 103-211.

Lieber, R.L., Jacobson, M.D., Fazeli, B.M., Abrams, R.A. and Botte, M.J. 1992. Architecture of selected muscles of the arm and forearm: anatomy and implications for tendon transfer. *The Journal of Hand Surgery* 17A (3), 787-798.

Lieber, R.L., Ljung, B.O. and Fridén, J. 1997. Intraoperative sarcomere length measurements reveal differential design of human wrist extensor muscles. *Journal of Experimental Biology* 200, 19-25.

Lopes, M. M. 2007. *Ultrasound measures of the carpal tunnel, tendon and nerve excursion*. Thesis (M.Sc.). York University.

Luopajärvi, T., Kuorinka, I., Virolainen, M. and Holmberg, M. 1979. Prevalence of tenosynovitis and other injuries of the upper extremities in repetitive work. *Scandinavian Journal of Work and Environmental Health* 5 (3), 48–55.

Manal, K. and Buchanan, T.S. 2004. Subject-specific estimates of tendon slack length: a numerical method. *Journal of Applied Biomechanics* 20, 195-203.

Manktelow, R.T., Binhammer, P., Tomat, L.R., Bril, V. and Szalai, J.P. 2004. Carpal tunnel syndrome: cross-sectional and outcome study in Ontario workers. *Journal of Hand Surgery* 29A (2), 307-317.

Marieb, E.N. 2003. Human Anatomy and Physiology. Sixth Edition. Pearson. San Francisco, CA.

Marras, W.S. and Schoenmarklin, R.W. 1993. Wrist motions in industry. *Journal of Ergonomics* 36 (4), 341-351.

Minamikawa, Y., Peimer, C.A., Yamaguchi, T., Banasiak, N.A., Kambe, K. and Sherwin, F.S. 1992. Wrist positions and extension tendon amplitude following repair. *Journal of Hand Surgery* 17A, 268-271.

Mogk, J.P.M. and Keir, P.J. 2007. Modelling extrinsic finger flexor tendon kinematics. Proceedings of the 29th Annual Meeting of the American Society of Biomechanics, Cleveland, Ohio.

Moore, A., Wells, R. and Ranney, D. 1991. Quantifying exposure in occupational manual tasks with cumulative trauma disorder potential. *Journal of Ergonomics* 34 (12), 1433-1453.

Moore, J.S. and Garg, A. 1994. A comparison of different approaches for ergonomic job evaluation for predicting risk of upper extremity disorders. IEA 94. Occupational Health and Safety *2*.

Nelson, J.E., Treaster, D.E. and Marras, W.S. 2000. Finger motion, wrist motion and tendon travel as a function of keyboard angles. *Clinical Biomechanics* 15, 489-498.

Netscher, D., Dinh, T., Cohen, V. and Thornby, J. 1998. Division of the transverse carpal ligament and flexor tendon excursion: open and endoscopic carpal tunnel release. *Plastic and Reconstructive Surgery* 102 (3), 773-778.

Netscher, D., Mosharrafa, A., Lee, M., Polsen, C., Choi, H., Steadman, A.K. and Thornby, J. 1997. Transverse carpal ligament: its effect on flexor tendon excursion, morphologic changes of the carpal canal, and on pinch and grip strengths after open carpal tunnel release. *Plastic and Reconstructive Surgery* 100 (3), 636-642.

NIOSH Publication. 1997. Chapter 5 Hand/Wrist Musculoskeletal Disorders (Carpal Tunnel Syndrome, Hand/Wrist Tendinitis, and Hand-Arm Vibration Syndrome): Evidence for Work-Relatedness. No. 97-141.

Oh, S., Belohlavek, M., Zhao, C., Osamura, N., Zobitz, M.E. and An, K. 2007. Detection of differential gliding characteristics of the flexor digitorum superficialis tendon and subsynovial connective tissue using color Doppler sonographic imaging. *Journal of Ultrasound Medicine* 26, 149-155.

Rempel, D., Bach, J.M., Gordon, L. and So, Y. 1998. Effects of forearm pronation/supination on carpal tunnel pressure. *Journal of Hand Surgery* 23A, 38-42.

Rempel, D., Keir, P.J., Smutz, W.P. and Hargens, A. 1997. Effects of static fingertip loading on carpal tunnel pressure. *Journal of Orthopaedic Research* 15 (3), 422-426.

Rettig, A.C. 2001. Wrist and hand overuse syndromes. *Clinics in Sports Medicine* 20 (3), 591-611.

Schneck, D.J. and Bronzino, J.D. 2003. Biomechanics: Principles and Applications. First Edition. CRC Press. New York, NY.

Schuind, F., Ventura, M. and Pasteels, J.L. 1990. Idiopathic carpal tunnel syndrome: histologic study of the flexor synovium. *Journal of Hand Surgery* 15A: 497-503.

Siegel, D.B., Kuzma, G. and Eakins, D. 1995. Anatomic investigation of the role of the lumbrical muscles in carpal tunnel syndrome. *Journal of Hand Surgery* 20A, 860-863.

Silverstein, B.A., Fine, L.J. and Armstrong, T.J. 1987. Occupational factors and the carpal tunnel syndrome. *American Journal of Industrial Medicine* 11 (3), 343– 358.

Silverstein, B., Welp, E., Nelson, N. and Kalat, J. 1998. Claims incidence of work-related disorders of the upper extremities: Washington State, 1987 through 1995. *American Journal of Public Health* 88 (12), 1827-1833.

Sommerich, C.M., Marras, W.S. and Parnianpour, M. 1996. A quantitative description of typing biomechanics. *Journal of Occupational Rehabilitation* 6 (1), 33-55.

Szabo, R.M., Bay, B.K., Sharkey, N.A. and Gaut, C. 1994. Median nerve displacement through the carpal tunnel. *Journal of Hand Surgery* 19A, 901-906.

Szabo, R.M. and Chidgey, L.K. 1989. Stress carpal tunnel pressures in patients with carpal tunnel syndrome and normal patients. *Journal of Hand Surgery* 14A, 624-627.

Tanaka, S., Petersen, M. and Cameron, L. 2001. Prevalence and risk factors of tendinitis and related disorders of the distal upper extremity among U.S. workers: comparison to carpal tunnel syndrome. *American Journal of Industrial Medicine* 39, 328-335.

Tanaka, S., Wild, D.K., Seligman, P.J., Halperin, W.E., Behrens, V.J. and Putz-Anderson, V. 1995. Prevalence of work-related carpal tunnel syndrome among U.S. workers: analysis of the occupational health supplement data of 1988 National Health Interview Survey. *American Journal of Industrial Medicine* 27 (4), 451–470.

Treaster, D.E. and Marras, W.S. 2000. An assessment of alternate keyboards using finger motion, wrist motion and tendon travel. *Clinical Biomechanics* 15, 499-503.

Uchiyama, S., Coert, J.H., Berglund, L., Amadio, P.C. and An, K.N. 1995. Method for the measurement of friction between tendon and pulley. *Journal of Orthopaedic Research* 13 (1), 83-89.

Ugbolue, U.C., Hsu, W., Goitz, R.J., Zong-Ming, L. 2005. Tendon and nerve displacement at the wrist during finger movements. *Clinical Biomechanics* 20, 50-56.

Valero-Cuevas, F.J., Zajac, F.E. and Burgar, C.G. 1998. Larger index fingertip forces are produced by subject-independent patterns of muscle excitation. *Journal of Biomechanics* 31, 693-703.

Vilimek, M. 2006. A numerical approach in estimation of tendon slack length in individual lower extremity muscles. Proceedings of the 30th Annual American Society for Biomechanics Meeting, Virginia Tech, Blacksburg, VA.

Weiss, N.D., Gordon, L., Bloom, T., So, Y. and Rempel, D.M. 1995. Positions of the wrist associated with the lowest carpal-tunnel pressure: implications for splint design. *Journal of Bone and Joint Surgery* 77(11), 1695-1699.

Werner, R.A., Franzblau, A., Gell, N., Ulin, S.S. and Armstrong, T.J. 2005. A longitudinal study of industrial and clerical workers: predictors of upper extremity tendonitis. *Journal of Occupational Rehabilitation* 15 (1), 37-46.

Winby, C.R., Lloyd, D.G. and Kirk, T.B. 2008. Evaluation of different analytical methods for subject-specific scaling of musculotendon parameters. *Journal of Biomechanics* 41, 1682-1688.

Workplace Safety & Insurance Board Of Ontario, 2006. *Statistical supplement of the 2006 annual report* [online]. Workplace Safety & Insurance Board Of Ontario. Available from: http://www.wsib.on.ca/wsib/wsibsite.nsf/Public/Statistics [Accessed 16 September 2008].

Wu, J.Z., An, K.N., Cutlip, R.G., Andrew, M.E. and Dong, R.G. 2009. Modelling of the muscle/tendon excursions and moment arms in the thumb using the commercial software anybody. *Journal of Biomechanics* 42, 383-388.

Yamaguchi, T., Osamura, N., Zhao, C., An, K.N. and Amadio, P.C. 2008. Relative longitudinal motion of the finger flexors, subsynovial connective tissue, and median nerve before and after carpal tunnel release in a human cadaver model. *Journal of Hand Surgery* 33A, 888-892.

Yoshii, Y., Zhao, C., Henderson, J., Zhao, K.D., Zobitz, M.E., An, K.N. and Amadio, P.C. 2008. Effects of carpal tunnel release on the relative motion of the tendon, nerve, and subsynovial connective tissue in a human cadaver model. *Clinical Biomechanics* 23, 1121-1127.

Zajac, F.E. 1989. Muscle and tendon: properties, models, scaling and application to biomechanics and motor control. *Critical Reviews in Biomedical Engineering* 17 (4), 359-411.

Zakaria, D. 2004. Rates of carpal tunnel syndrome, epicondylitis, and rotator cuff claims in Ontario workers during 1997. *Chronic Diseases in Canada* 25 (2), 32-39.

Zakaria, D., Robertson, J., Koval, J., MacDermid, J. and Hartford, K. 2004. Rates of claims for cumulative trauma disorder of the upper extremity in Ontario workers during 1997. *Chronic Diseases in Canada* 25 (1), 22-31.

Zhao, C., Ettema, A.M., Osamura, N., Berglund, L.J., An, K.N and Amadio, P.C. 2007. Gliding characteristics between flexor tendons and surrounding tissues in the carpal tunnel: a biomechanical cadaver study. *Journal of Orthopaedic Research* 25, 185-190.

APPENDIX A: TENDON EXCURSION AND MOMENT ARM RMSD

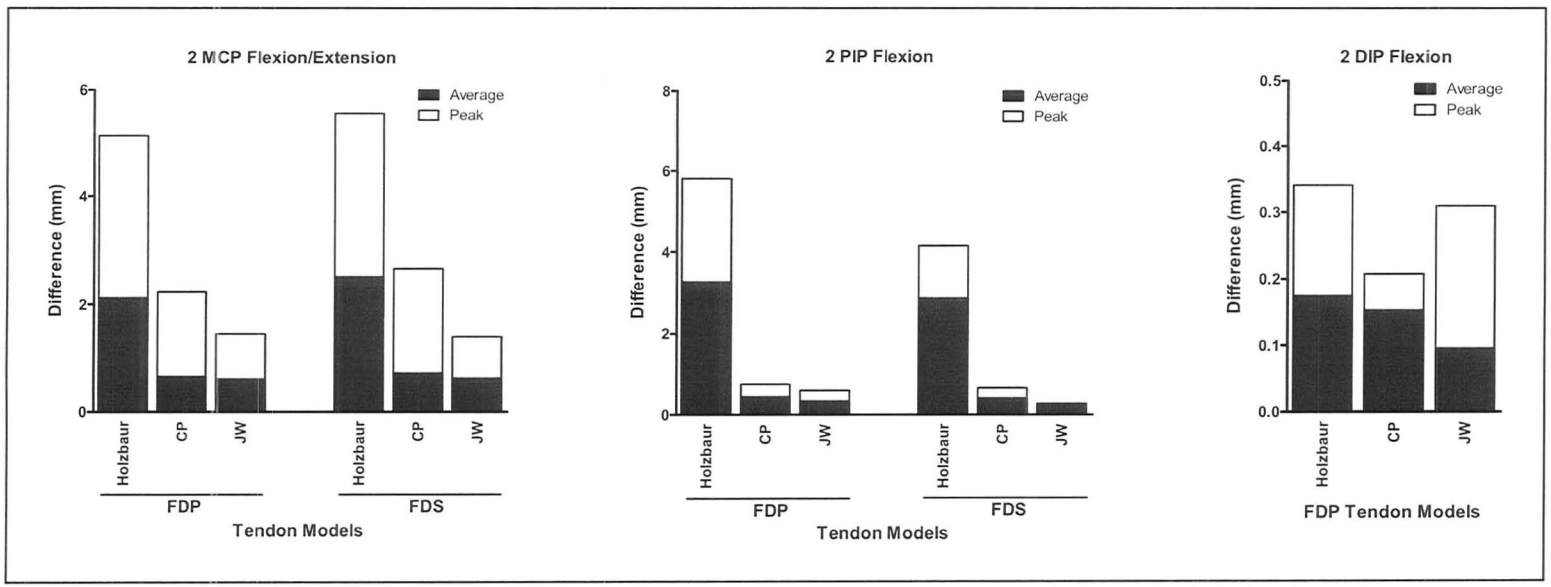

Figure A.1. FDPi and FDSi tendon excursion RMSD of the musculoskeletal models compared to the anthropometric regression model developed by Armstrong and Chaffin (1978). Holzbaur – Holzbaur et al. (2005) model; CP – Control point model; JW – Joint wrapping model.

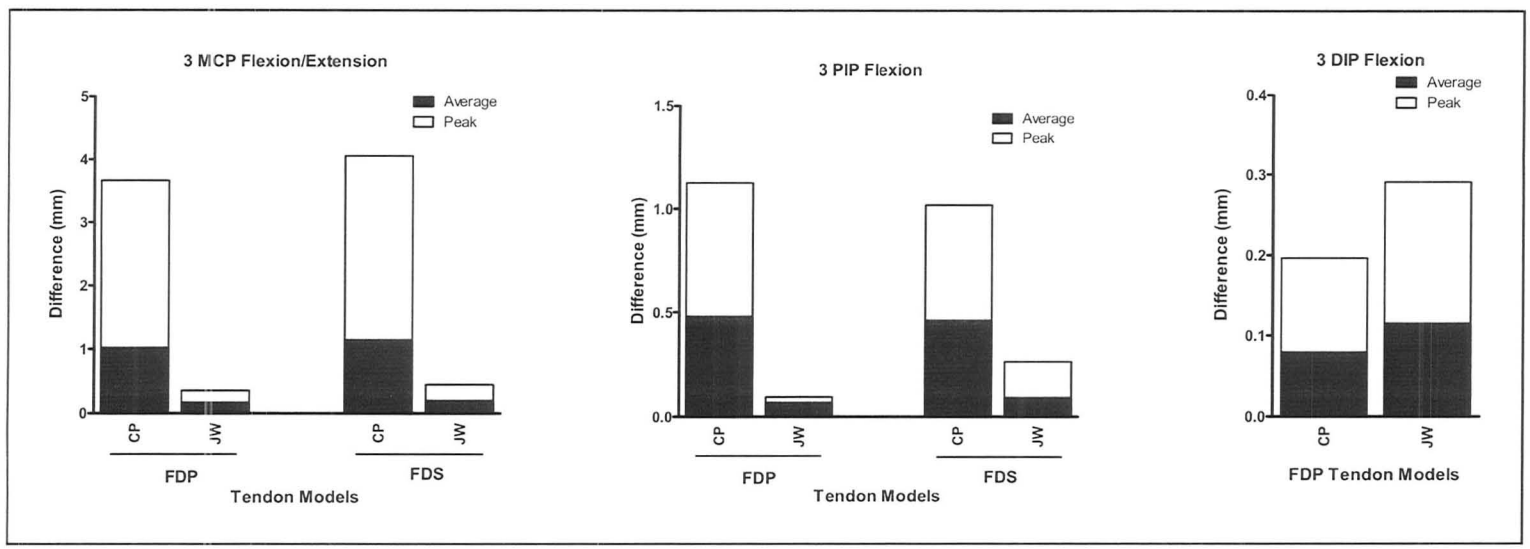

Figure A.2. FDPm and FDSm tendon excursion RMSD of the musculoskeletal models compared to the anthropometric regression model developed by Armstrong and Chaffin (1978). CP – Control point model; JW – Joint wrapping model.

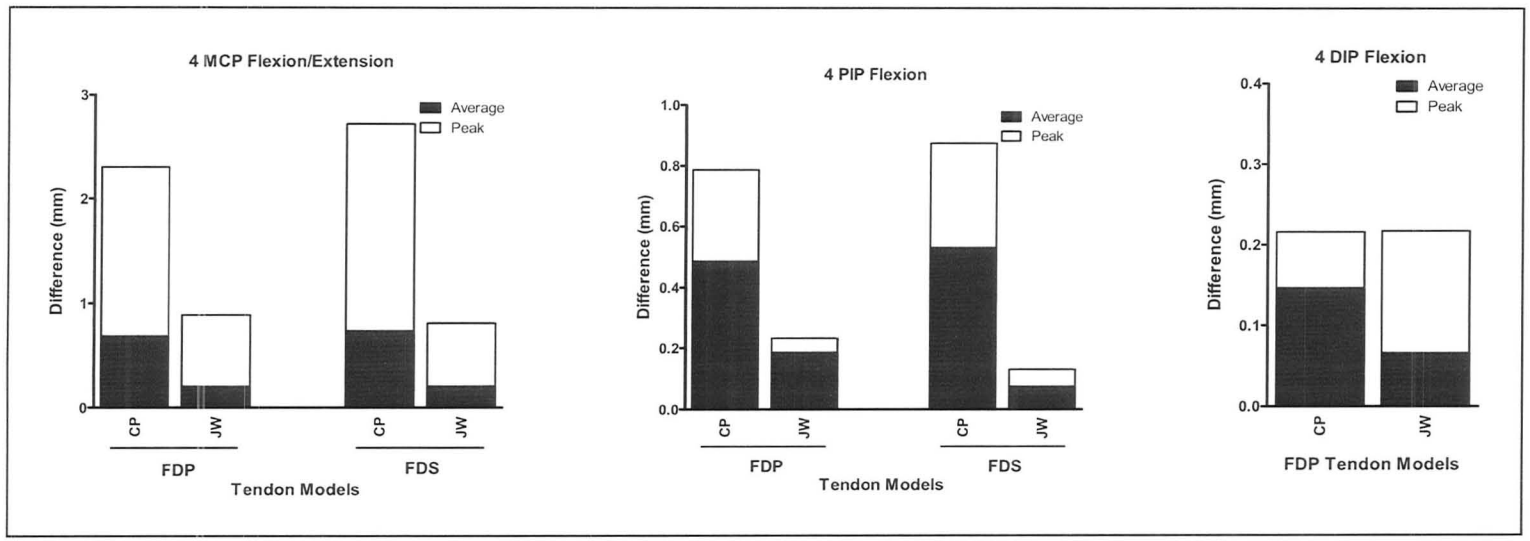

Figure A.3. FDPr and FDSr tendon excursion RMSD of the musculoskeletal models compared to the anthropometric regression model developed by Armstrong and Chaffin (1978). CP – Control point model; JW – Joint wrapping model.

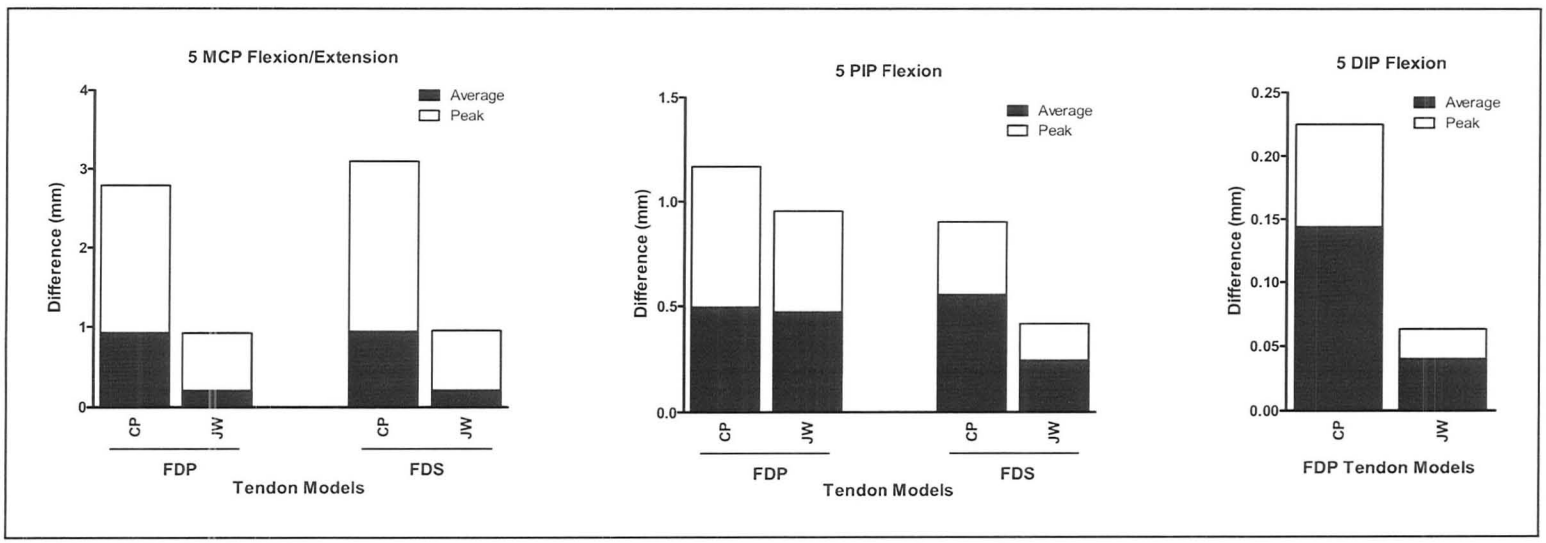

Figure A.4. FDPl and FDSl tendon excursion RMSD of the musculoskeletal models compared to the anthropometric regression model developed by Armstrong and Chaffin (1978). CP – Control point model; JW – Joint wrapping model.

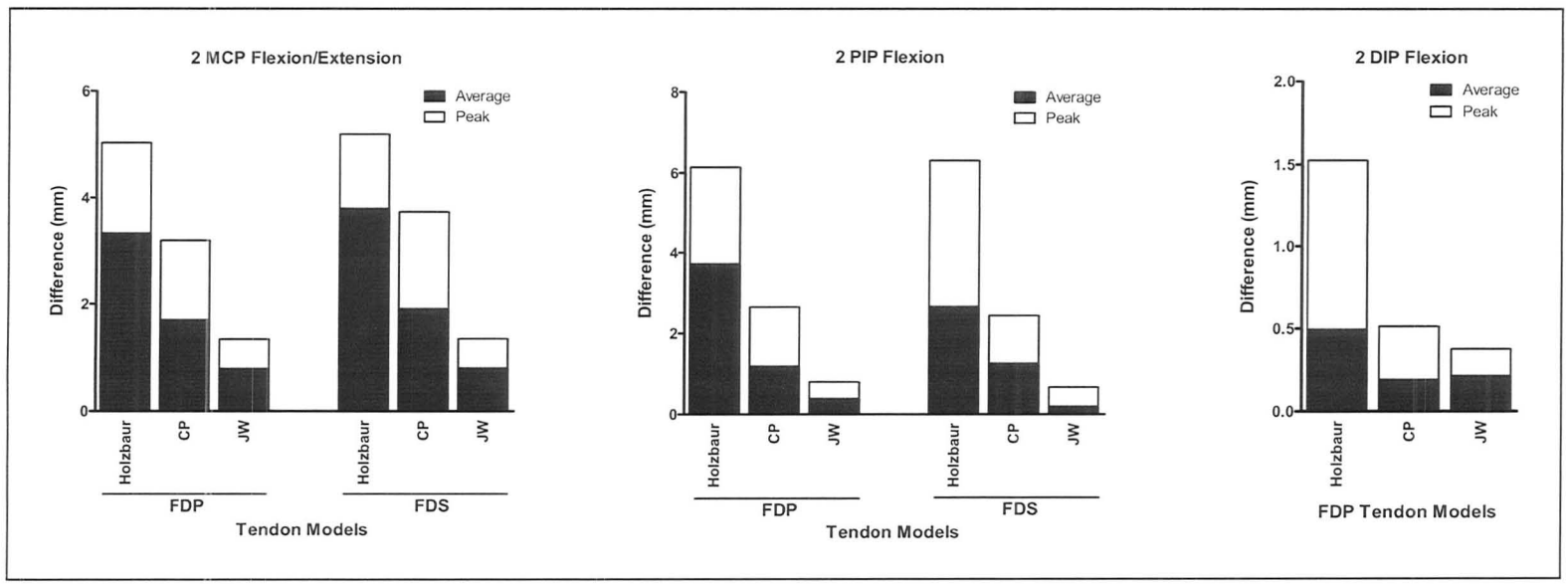

Figure A.5. FDPi and FDSi moment arm RMSD of the musculoskeletal models compared to the anthropometric regression model developed by Armstrong and Chaffin (1978). Holzbaur – Holzbaur et al. (2005) model; CP – Control point model; JW – Joint wrapping model.

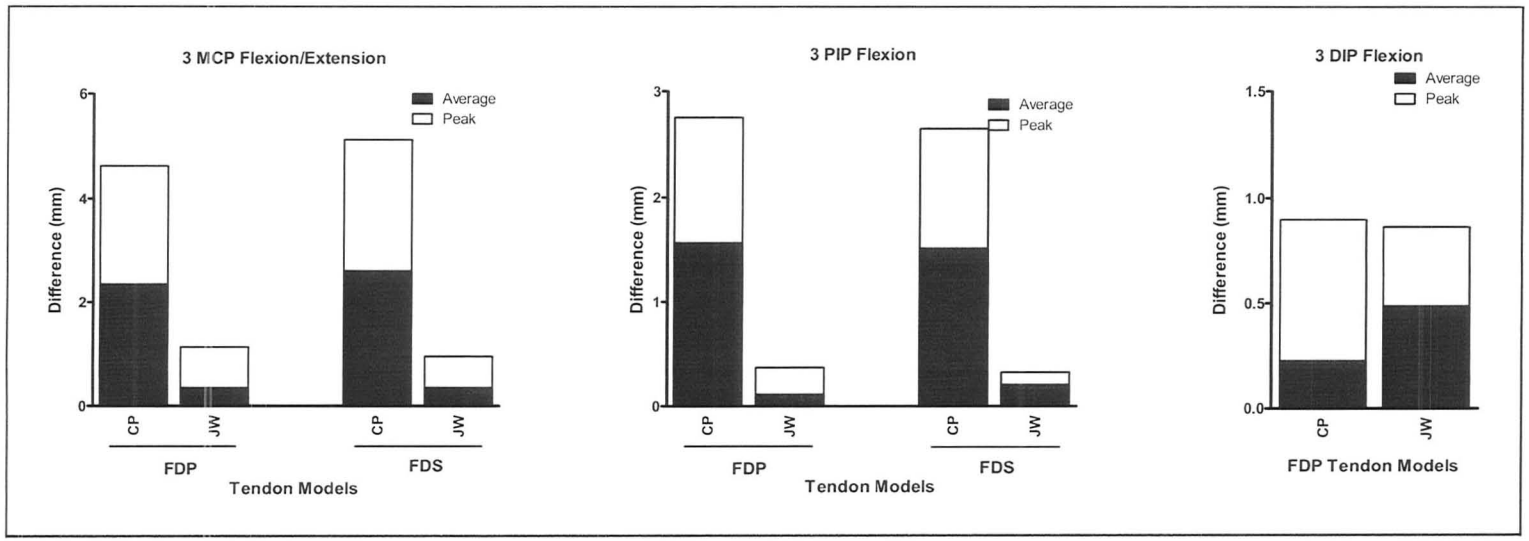

Figure A.6. FDPm and FDSm moment arm RMSD of the musculoskeletal models compared to the anthropometric regression model developed by Armstrong and Chaffin (1978). CP – control point model; JW – joint wrapping model.

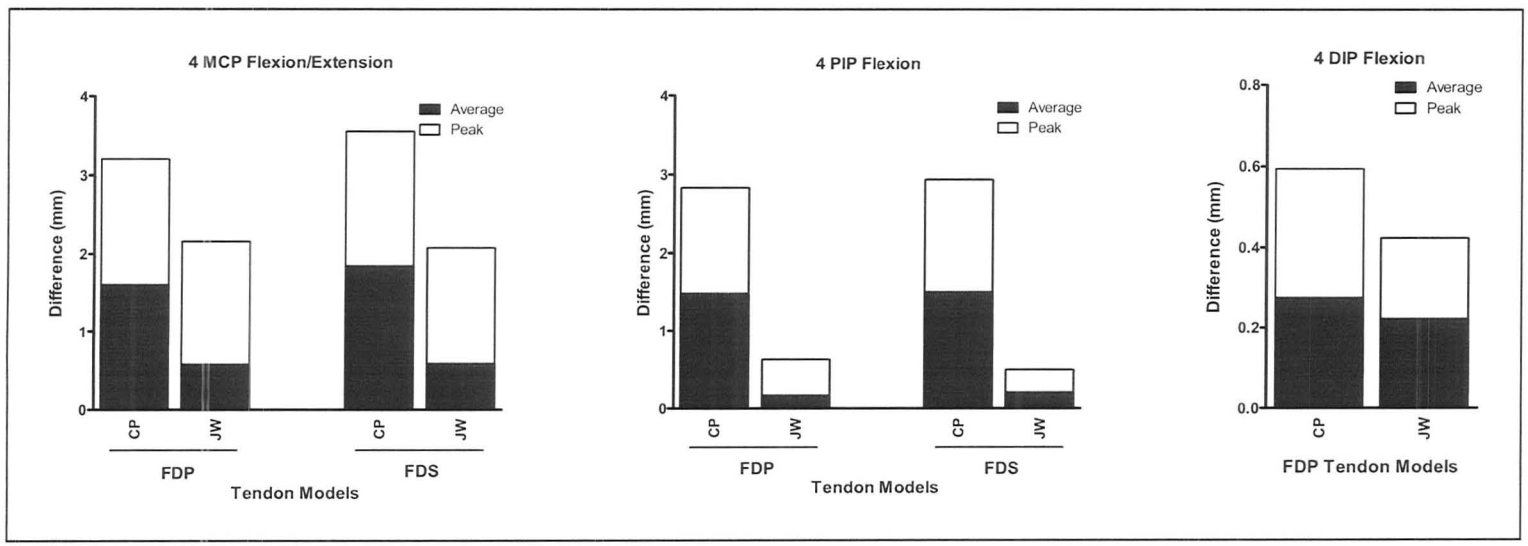

Figure A.7. FDPr and FDSr moment arm RMSD of the musculoskeletal models compared to the anthropometric regression model developed by Armstrong and Chaffin (1978). CP – Control point model; JW – Joint wrapping model.

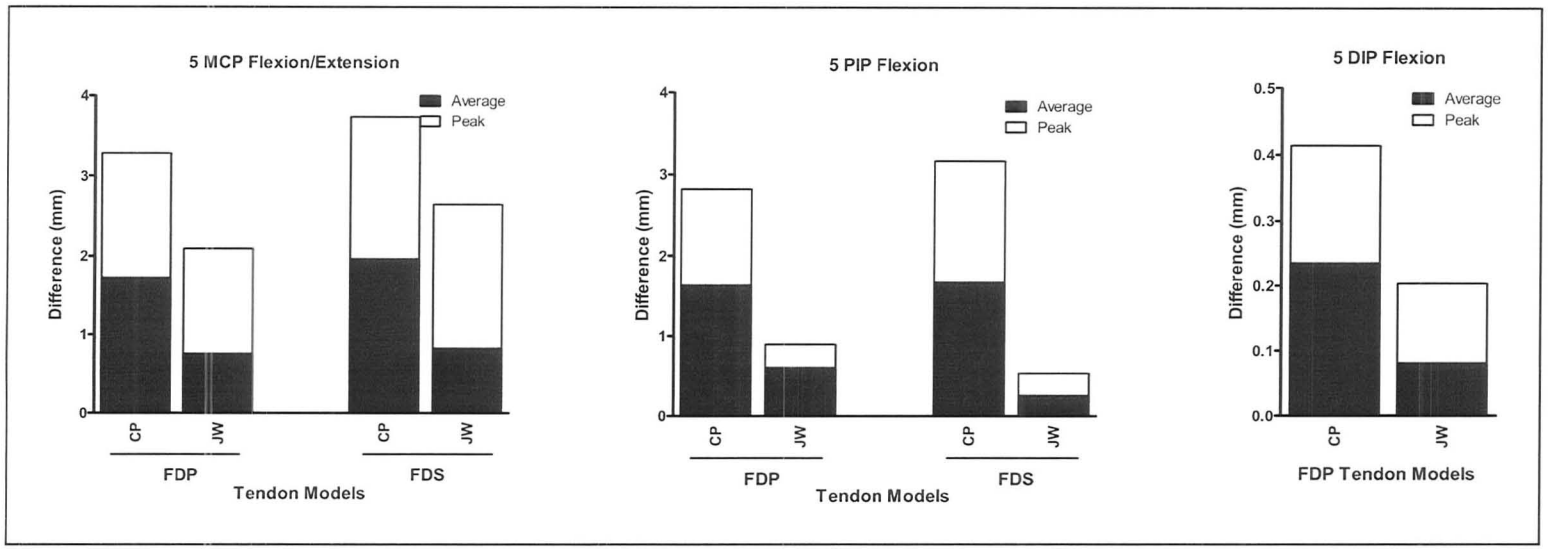

Figure A.8. FDPl and FDSl moment arm RMSD of the musculoskeletal models compared to the anthropometric regression model developed by Armstrong and Chaffin (1978). CP – Control point model; JW – Joint wrapping model.

APPENDIX B: TENDON EXCURSIONS AND MOMENT ARMS WITH ANTHROPOMETRIC SCALING

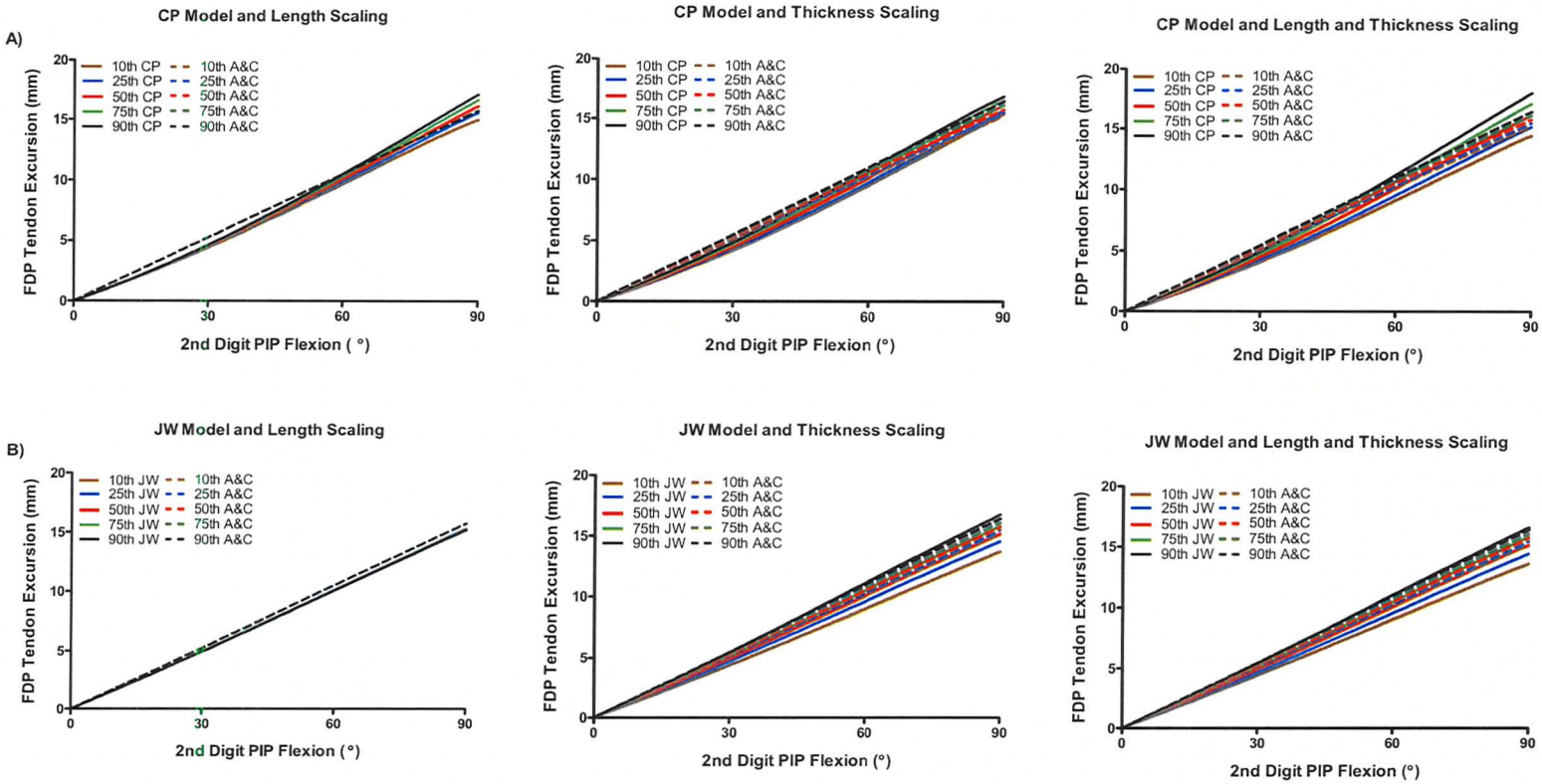

Figure B.1. FDPi tendon excursions with phalangeal length scaling (left), thickness scaling (centre) and length and thickness scaling (right). CP – Control point model; JW – Joint wrapping model; A&C – Armstrong and Chaffin (1978) regression model. Anthropometrical scaling corresponds to dimensions for 10th, 25th, 50th, 75th and 90th percentile males.

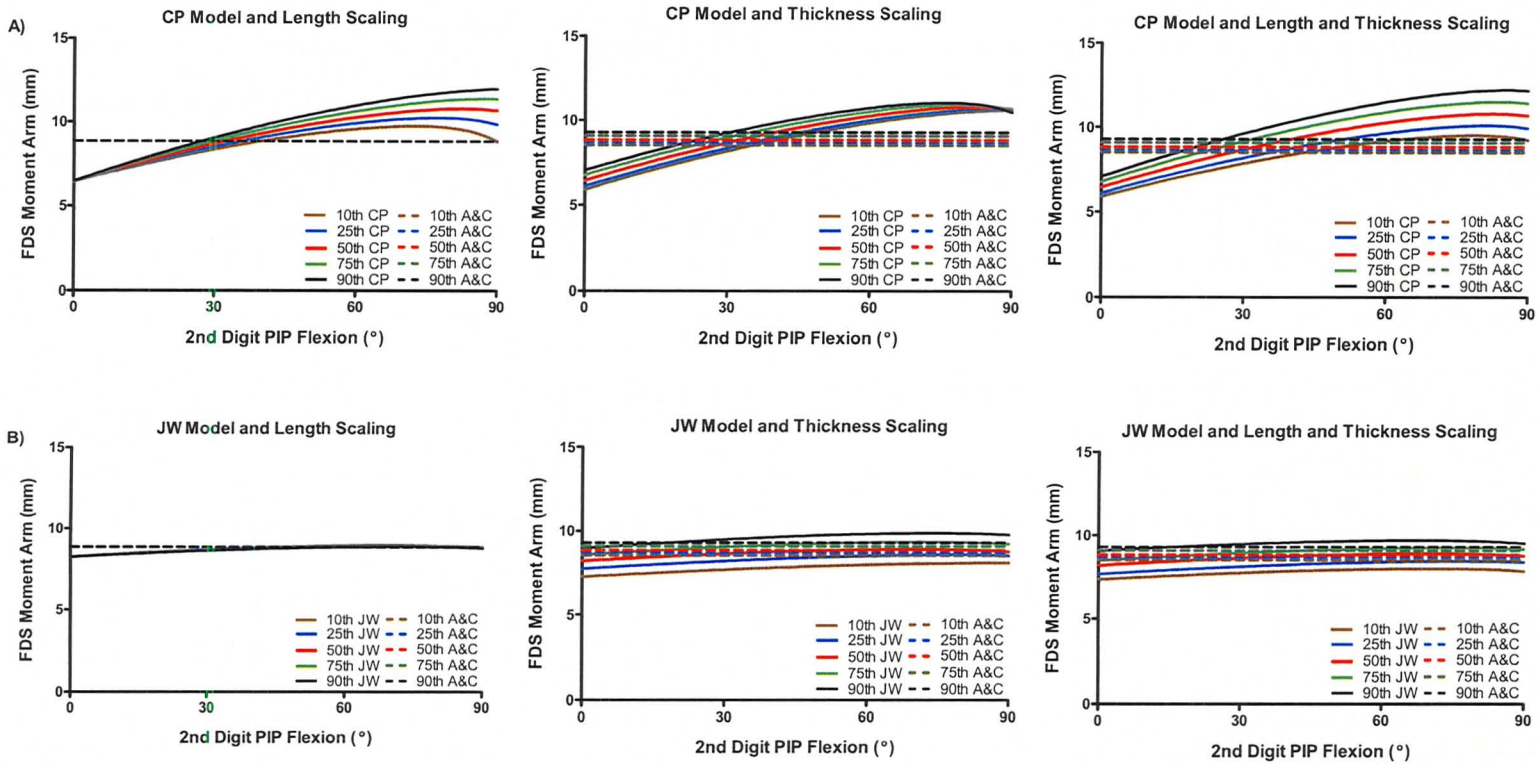

Figure B.2. FDSi moment arms with phalangeal length scaling (left), thickness scaling (centre) and length and thickness scaling (right). CP – Control point model; JW – Joint wrapping model; A&C – Armstrong and Chaffin (1978) regression model. Anthropometrical scaling corresponds to dimensions for 10^{th}, 25^{th}, 50^{th}, 75^{th} and 90^{th} percentile males.

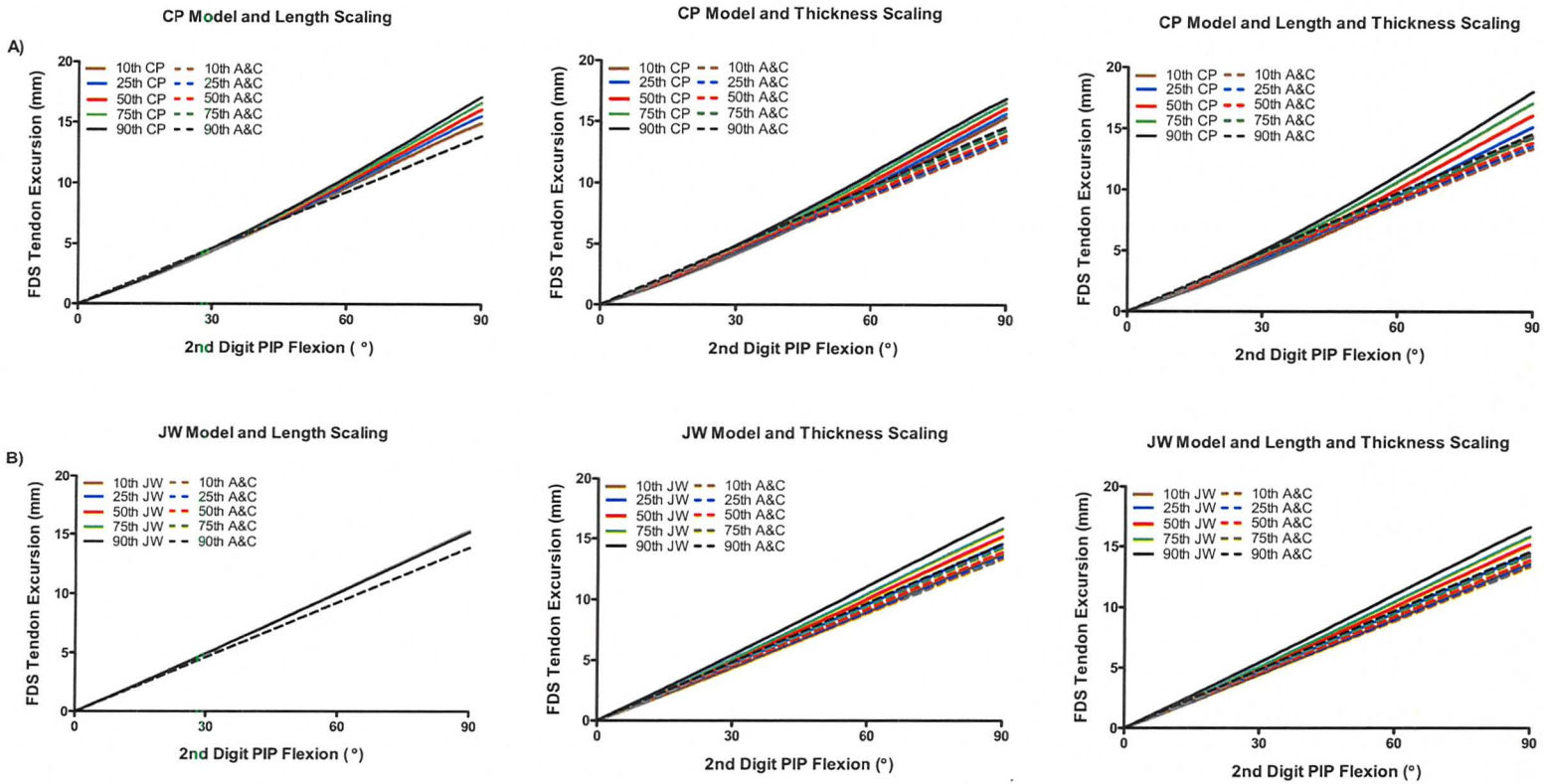

Figure B.3. FDSi tendon excursions with phalangeal length scaling (left), thickness scaling (centre) and length and thickness scaling (right). CP – Control point model; JW – Joint wrapping model; A&C – Armstrong and Chaffin (1978) regression model. Anthropometrical scaling corresponds to dimensions for 10th, 25th, 50th, 75th and 90th percentile males.

APPENDIX C: EXPERIMENTALLY MEASURED HAND DIMENSIONS AND MOMENT ARMS

Table C.1. Experimentally measured segment lengths of the index, middle, ring and little fingers measured with calipers in mm (percentile rankings in brackets).

		Index Finger			Middle Finger			Ring Finger			Little Finger		
Participant	**Sex**	**PP**	**MP**	**DP**	**PP**	**MP**	**DP**	**PP**	**MP**	**DP**	**PP**	**MP**	**DP**
1	**M**	54(13)	24(7)	29(60)	64(97)	28(72)	31(87)	61(98)	28(92)	30(57)	47(94)	17(41)	26(28)
2	**F**	46(1)	20(14)	22(1)	48(9)	21(3)	23(1)	47(5)	20(5)	23(1)	34(2)	14(3)	22(1)
3	**M**	50(3)	25(84)	26(15)	57(67)	27(58)	27(27)	55(70)	24(46)	28(25)	45(83)	20(87)	24(8)
Average		**50(6)**	**23(57)**	**26(25)**	**56(58)**	**25(44)**	**27(38)**	**54(58)**	**24(48)**	**27(27)**	**42(60)**	**17(44)**	**24(12)**
Standard Deviation		**4(6)**	**3(38)**	**4(31)**	**8(44)**	**4(37)**	**4(44)**	**7(47)**	**4(44)**	**4(28)**	**7(50)**	**3(42)**	**2(14)**

* PP - proximal phalanx; MP - middle phalanx; DP - distal Phalanx

Table C.2. Experimentally measured joint thicknesses of the index, middle, ring and little fingers measured with calipers in mm (percentile rankings in brackets).

		Index Finger			Middle Finger			Ring Finger			Little Finger		
Participant	**Sex**	**MCP**	**PIP**	**DIP**	**MCP**	**PIP**	**DIP**	**MCP**	**PIP**	**DIP**	**MCP**	**PIP**	**DIP**
1	**M**	28	19(37)	14(13)	31	21(74)	15(22)	27	19(53)	13(54)	24	16(28)	12(10)
2	**F**	20	15(1)	11(1)	21	14(1)	12(1)	22	14(1)	11(1)	18	12(1)	10(1)
3	**M**	27	18(12)	14(13)	28	19(22)	15(22)	27	18(25)	13(22)	25	16(28)	14(59)
Average		**25**	**17(16)**	**13(8)**	**27**	**18(32)**	**14(15)**	**25**	**17(26)**	**12(9)**	**22**	**15(19)**	**12(23)**
Standard Deviation		**4**	**2(19)**	**2(7)**	**5**	**4 (38)**	**2(13)**	**3**	**3(27)**	**1(12)**	**4**	**2(16)**	**2(32)**

* MCP - metacarpophalangeal; PIP - proximal interphalangeal; DIP - distal interphalangeal

Table C.3. Experimentally measured extrinsic finger flexor moment arms (from ultrasound images) of the index, middle, ring and little finger joints in neutral posture (mm).

			Index Finger			Middle Finger			Ring Finger			Little Finger		
Participant	**Sex**	**Tendon**	**MCP**	**PIP**	**DIP**	**MCP**	**PIP**	**DIP**	**MCP**	**PIP**	**DIP**	**MCP**	**PIP**	**DIP**
1	**M**	**FDP**	9.3	10.0	7.3	10.4	10.6	7.7	9.3	9.3	6.2	8.9	8.1	5.4
		FDS	11.0	8.7	-	12.3	9.6	-	10.6	8.3	-	10.4	7.5	-
2	**F**	**FDP**	7.7	8.9	5.6	8.1	8.9	6.0	8.1	7.7	5.2	7.1	6.9	4.4
		FDS	9.3	7.5	-	9.6	7.5	-	9.3	6.6	-	7.9	6.0	-
3	**M**	**FDP**	8.1	9.8	6.4	9.3	10.0	6.6	8.1	9.8	6.4	7.7	7.9	5.4
		FDS	9.8	8.5	-	11.0	8.7	-	9.8	8.5	-	9.1	7.1	-
Average (SD)		**FDP**	**8.4 (1.1)**	**9.6 (0.8)**	**6.4 (1.2)**	**9.3 (1.6)**	**9.8 (1.2)**	**6.8 (1.2)**	**8.5 (0.8)**	**8.9 (1.1)**	**5.9 (0.7)**	**7.9 (1.3)**	**7.6 (0.8)**	**5.1 (0.7)**
		FDS	**10.0 (0.9)**	**8.3 (0.6)**	**- -**	**11.0 (1.4)**	**8.6 (1.1)**	**- -**	**9.9 (0.7)**	**8.0 (1.0)**	**- -**	**9.1 (1.3)**	**6.9 (0.8)**	**- -**

* MCP - metacarpophalangeal; PIP - proximal interphalangeal; DIP - distal interphalangeal

APPENDIX D: REGRESSIONS OF HAND DIMENSIONS AND MOMENT ARMS

Model Summary[b]

Model	R	R Square	Adjusted R Square	Std. Error of the Estimate	Durbin-Watson
1	.815[a]	.663	.630	.57798	1.295

a. Predictors: (Constant), MCP_T

b. Dependent Variable: MCP_MA

ANOVA[b]

Model		Sum of Squares	df	Mean Square	F	Sig.
1	Regression	6.587	1	6.587	19.716	.001[a]
	Residual	3.341	10	.334		
	Total	9.927	11			

a. Predictors: (Constant), MCP_T

b. Dependent Variable: MCP_MA

Coefficients[a]

Model		Unstandardized Coefficients		Standardized Coefficients	t	Sig.
		B	Std. Error	Beta		
1	(Constant)	3.566	1.128		3.163	.010
	MCP_T	.199	.045	.815	4.440	.001

a. Dependent Variable: MCP_MA

Figure D.1. Linear regression analysis relating MCP joint thicknesses (the predictor) and FDP moment arms (the criterion).

Model Summary[b]

Model	R	R Square	Adjusted R Square	Std. Error of the Estimate	Durbin-Watson
1	.913[a]	.833	.816	.48480	1.368

a. Predictors: (Constant), PIP_T

b. Dependent Variable: PIP_MA

ANOVA[b]

Model		Sum of Squares	df	Mean Square	F	Sig.
1	Regression	11.731	1	11.731	49.912	.000[a]
	Residual	2.350	10	.235		
	Total	14.081	11			

a. Predictors: (Constant), PIP_T

b. Dependent Variable: PIP_MA

Coefficients[a]

Model		Unstandardized Coefficients		Standardized Coefficients	t	Sig.
		B	Std. Error	Beta		
1	(Constant)	2.268	.961		2.360	.040
	PIP_T	.399	.056	.913	7.065	.000

a. Dependent Variable: PIP_MA

Figure D.2. Linear regression analysis relating PIP joint thicknesses (the predictor) and FDP moment arms (the criterion).

Model Summary[b]

Model	R	R Square	Adjusted R Square	Std. Error of the Estimate	Durbin-Watson
1	.813[a]	.661	.627	.56725	2.319

a. Predictors: (Constant), DIP_T

b. Dependent Variable: DIP_MA

ANOVA[b]

Model		Sum of Squares	df	Mean Square	F	Sig.
1	Regression	6.263	1	6.263	19.466	.001[a]
	Residual	3.218	10	.322		
	Total	9.481	11			

a. Predictors: (Constant), DIP_T

b. Dependent Variable: DIP_MA

Coefficients[a]

Model		Unstandardized Coefficients		Standardized Coefficients	t	Sig.
		B	Std. Error	Beta		
1	(Constant)	.607	1.247		.487	.637
	DIP_T	.428	.097	.813	4.412	.001

a. Dependent Variable: DIP_MA

Figure D.3. Linear regression analysis relating DIP joint thicknesses (the predictor) and FDP moment arms (the criterion).

Model Summary[b]

Model	R	R Square	Adjusted R Square	Std. Error of the Estimate	Durbin-Watson
1	.857[a]	.734	.707	.61005	1.293

a. Predictors: (Constant), MCP_T

b. Dependent Variable: MCP_MA

ANOVA[b]

Model		Sum of Squares	df	Mean Square	F	Sig.
1	Regression	10.248	1	10.248	27.537	.000[a]
	Residual	3.722	10	.372		
	Total	13.970	11			

a. Predictors: (Constant), MCP_T

b. Dependent Variable: MCP_MA

Coefficients[a]

Model		Unstandardized Coefficients		Standardized Coefficients	t	Sig.
		B	Std. Error	Beta		
1	(Constant)	3.830	1.190		3.218	.009
	MCP_T	.249	.047	.857	5.248	.000

a. Dependent Variable: MCP_MA

Figure D.4. Linear regression analysis relating MCP joint thicknesses (the predictor) and FDS moment arms (the criterion).

Model Summary[b]

Model	R	R Square	Adjusted R Square	Std. Error of the Estimate	Durbin-Watson
1	.969[a]	.939	.933	.26385	2.035

a. Predictors: (Constant), PIP_T

b. Dependent Variable: PIP_MA

ANOVA[b]

Model		Sum of Squares	df	Mean Square	F	Sig.
1	Regression	10.652	1	10.652	153.009	.000[a]
	Residual	.696	10	.070		
	Total	11.348	11			

a. Predictors: (Constant), PIP_T

b. Dependent Variable: PIP_MA

Coefficients[a]

Model		Unstandardized Coefficients		Standardized Coefficients	t	Sig.
		B	Std. Error	Beta		
1	(Constant)	1.476	.523		2.823	.018
	PIP_T	.380	.031	.969	12.370	.000

a. Dependent Variable: PIP_MA

Figure D.5. Linear regression analysis relating PIP joint thicknesses (the predictor) and FDS moment arms (the criterion).

APPENDIX E: ISOMETRIC FORCE AND MOMENT CAPABILITIES

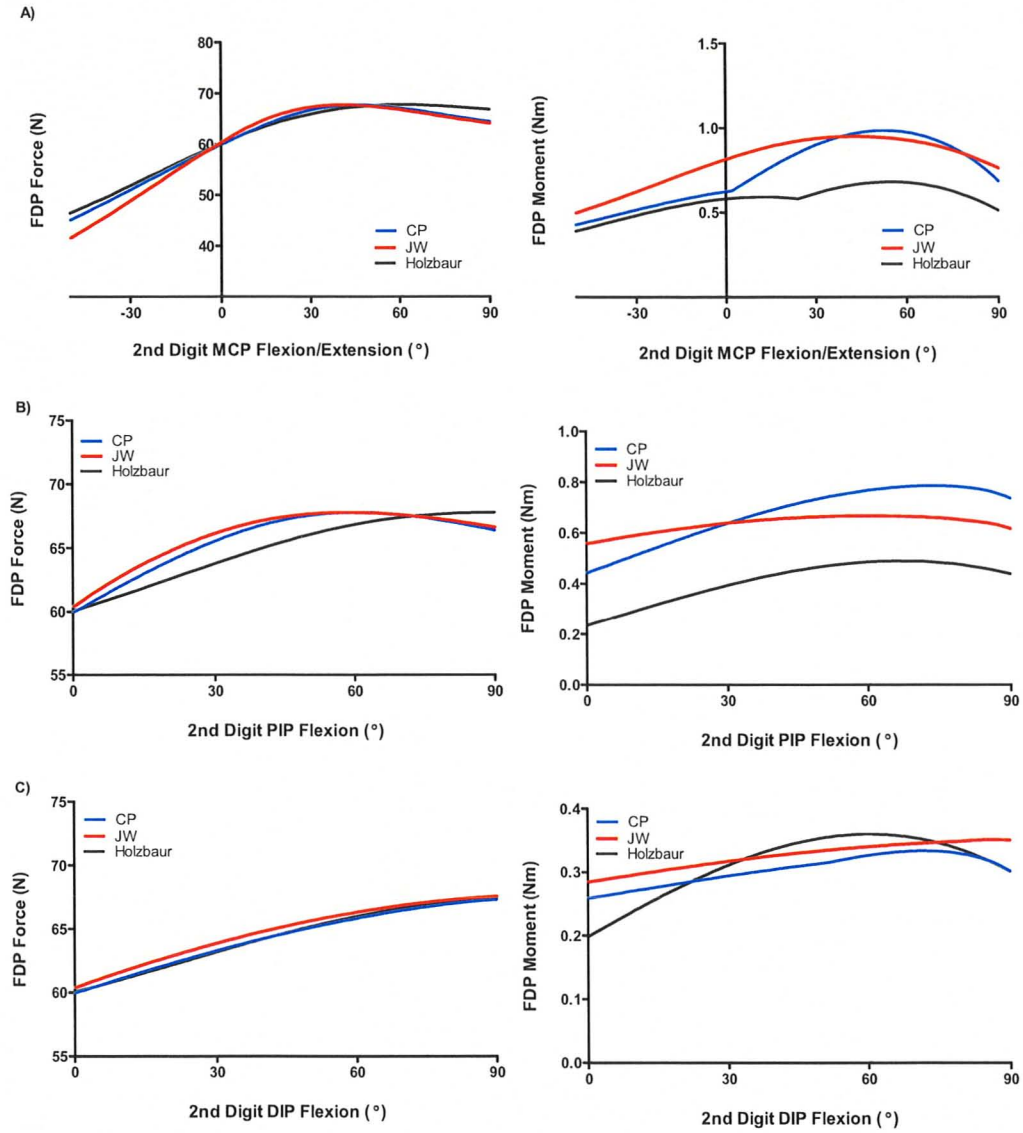

Figure E.1. Maximum isometric force (left) and moment (right) generating capabilities of the FDPi with index finger (a) MCP, (b) PIP and (c) DIP flexion/extension. CP – Control point model; JW – Joint wrapping model; Holzbaur - Holzbaur et al. (2005) model

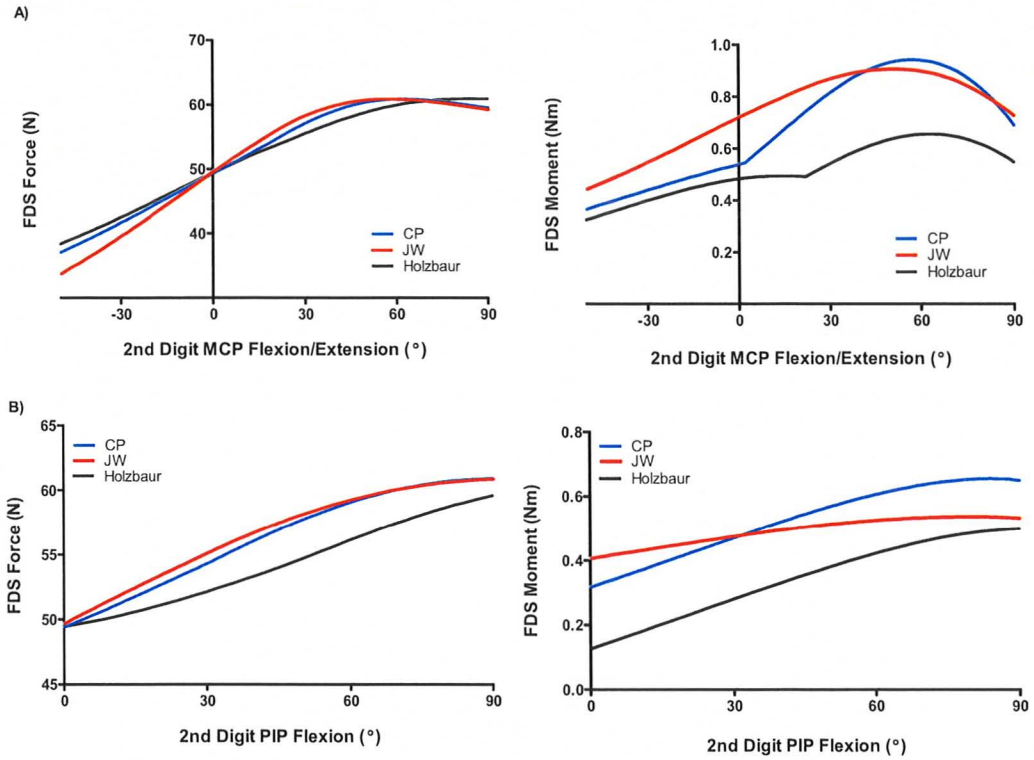

Figure E.2. Maximum isometric force (left) and moment (right) generating capabilities of the FDSi with index finger (a) MCP and (b) PIP flexion/extension. CP – Control point model; JW – Joint wrapping model; Holzbaur - Holzbaur et al. (2005) model